

Multi-responsive self-healing metallosupramolecular gels based on “click” ligand

Jinchun Yuan, Xiuli Fang, Lingxing Zhang, Guangning Hong, Yangju Lin, Qifeng Zheng, Yuanze Xu, Yonghong Ruan, Wengui Weng,* Haiping Xia, and Guohua Chen

Supporting Information

Table of Contents

I. Experimental Section

1.1 Materials

1.2 Safety Comments

1.3 Synthesis

1.3.1 Synthesis of **1**

1.3.2 Synthesis of **2**

1.3.3 Synthesis of **3**

1.3.4 Synthesis of **4**

1.3.5 Synthesis of **5**

1.4 UV Titration of **4** with Metal Ions

1.5 UV Titration of **Zn:4** and **Eu:4** with Solvents and Chemical

1.6 Swelling Tests of Gels

1.7 Optical Properties of Gels

1.8 Temperature Responsiveness of Gels

1.9 Chemical Responsiveness of Gels

1.10 Self-Healing of Coatings

II. Supplementary Results

III. References

I. Experimental Section

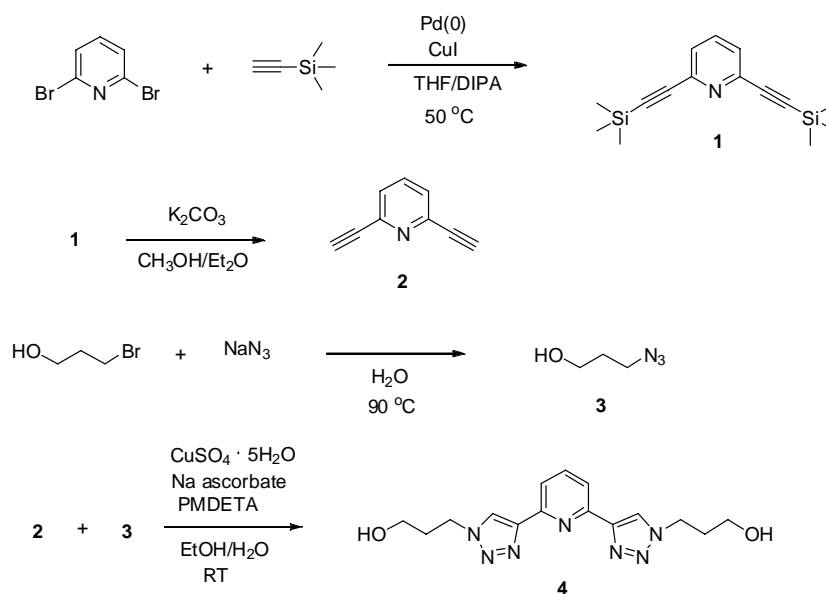
1.1 Materials

Solvents and chemicals were purchased from Sinopharm, Sigma-Aldrich, and Aladdin, and used as received unless otherwise noted. Toluene, dichloromethane (CH_2Cl_2), dimethyl sulfoxide (DMSO), dimethyl formamide (DMF), diisopropylamine (DIPA) were distilled under N_2 over CaH_2 , tetrahydrofuran (THF) over Na, prior to use.

1.2 Safety Comments

Sodium azide is very toxic, personal protection precautions should be taken. As low-molecular-weight organic azides are potential explosives, care must be taken during their handling. Generally, when the total number of carbon (n_C) plus oxygen (n_O) atoms is less than the total numbers of nitrogen atoms (n_N) by a ratio of three, that is, $(n_C+n_O)/n_N < 3$, the compound is considered as an explosive hazard. In these instances, the organic azido compound was prepared prior to use and used immediately.

1.3 Synthesis



Scheme S1. Synthesis of bis-hydroxy functionalized BTP ligand **4** using CuAAC click chemistry.

1.3.1 Synthesis of 1

1 was prepared according to literature^[1] with modifications. To a 50 ml flask was added 2.0 g (8.4

mmol, 1.0 eq) 2,6-dibromopyridine, 0.032 g (0.17 mmol, 0.02 eq) CuI, 0.195 g (0.17 mmol, 0.02 eq) Pd(PPh₃)₄, then evacuated at RT for 10 min and flushed with N₂, and 15 ml THF and 15 ml DIPA were added via a syringe under N₂. After freeze degassing (3x), TMS-acetylene, 2.92 ml (21.1 mmol, 2.5 eq) was added via a syringe in a counterflow of N₂. The reaction mixture was stirred at 50 °C for 6 h and after consumption of 2,6-dibromopyridine indicated by TLC monitoring (CH₂Cl₂/hexane 1/1) the mixture was cooled down to RT and the solvent was removed. Purification using column chromatography (CH₂Cl₂/hexane 1/1) gave 1.98 g (8.13 mmol, 98% yield) 2,6-bis(trimethylsilylethynyl)pyridine (**1**) as white powder. ¹H NMR (CDCl₃, 400 MHz): δ (ppm) = 7.58 (t, 1H, *J* = 8.0 Hz), 7.37 (d, 2H, *J* = 8.0 Hz), 0.25 (s, 18H).

1.3.2 Synthesis of 2

2 was prepared according to literature^[1] with modifications. To a flask was added 1.98 g (8.13 mmol, 1.0 eq) **1**, 3.36 g (24.4 mmol, 3.0 eq) K₂CO₃, and methanol (15 ml), diethyl ether (15 ml). The reaction was stirred at RT for 4 h and then additional diethyl ether (20 ml) and deionized water (30 ml) were added. After extracting with diethyl ether and deionized water for 3 more, the organic phase was collected and the solvent was removed. Purification using column chromatography (CH₂Cl₂/hexane 2/3) gave 0.68 g (5.37 mmol, 66% yield) 2,6-bis(ethynyl)pyridine (**2**). ¹H NMR (CDCl₃, 400 MHz): δ (ppm) = 7.65 (t, 1H, *J* = 7.8 Hz), 7.37 (d, 2H, *J* = 7.8 Hz), 3.16 (s, 2H).

1.3.3 Synthesis of 3

3 was prepared according to literature^[2] with modifications. To a mixture of 2.0 g (14.38 mmol, 1.0 eq) 3-bromo-1-propanol and 4.6 g (71.9 mmol, 5 eq) sodium azide was added 30 ml deionized water. After stirring and refluxing at 90 °C for 1 d, the product was extracted with CH₂Cl₂ (3x). The combined organic phases were dried over MgSO₄. After removal of the solvent in vacuo purification by column chromatography gave 1.38 g (13.6 mmol, 95% yield) 3-azido-1-propanol (**3**). ¹H NMR (CDCl₃, 400MHz): δ (ppm) = 3.74 (t, 2H, *J* = 6.0 Hz), 3.44 (t, 2H, *J* = 6.8 Hz), 1.82 (m, 2H).

1.3.4 Synthesis of 4

4 was prepared according to literature^[1b-e] with modifications. A solution of 0.50 g (3.93 mmol, 1.0 eq) **2**, 0.79 g (7.86 mmol, 2.0 eq) **3**, 0.098 g (0.39 mmol, 0.1 eq) CuSO₄·5H₂O, 0.46 g (2.3 mmol,

0.6 eq) sodium ascorbate, 0.245 ml (1.17 mmol, 0.3 eq) pentamethyldiethylenetriamine (PMDETA) in a 1:1 mixture of EtOH:H₂O was stirred at RT for 1 d. After removal of the solvents in vacuo, the crude product was purified by column chromatography (CH₂Cl₂:MeOH, 3:1) to afford 1.18 g (3.62 mmol, 92% yield) **4**. ¹H NMR (CDCl₃, 400 MHz): δ (ppm) = 8.23 (s, 2H), 8.08 (d, 2H, *J* = 8.0 Hz), 7.86 (t, 1H, *J* = 8.0 Hz), 4.61 (t, 4H, *J* = 6.4 Hz), 3.70 (t, 4H, *J* = 6.0 Hz), 2.24-2.17 (m, 4H).

1.3.5 Synthesis of **5**

5 was prepared according to literature^[31] with modifications. A mixture of PTHF (M_n = 2000, 3.0 g, 1.5 mmol, 1.0 eq) and DBTDL (10 μL, 0.01695 mmol, 0.0113 eq) in DMF (4 mL) was added dropwise in a time length of 30 min to a solution of HDI (485 μL, 3 mmol, 2 eq) in DMF (1 mL). The solution was stirred at 30 °C for 1 h, then a solution of **4** (494.0 mg, 1.0 eq) in DMF was added dropwise in a time length of 10 min. The solution was stirred at 30 °C for 1 d, resulting in a viscous solution. Precipitation from methanol provided crude polymer **5**, further dialysis over chloroform afforded clean polymer **5** (3.2 g, 80% yield). ¹H NMR(CDCl₃, 400 MHz): δ (ppm) = 8.33, 8.12, 7.91, 4.55-4.73, 4.16, 4.05, 3.65, 3.41, 3.14, 2.31, 2.20, 1.62, 1.47, 1.33. GPC (THF): M_n = 30000 g/mol, M_w = 45000 g/mol, PDI = 1.49.

1.4 UV Titration of **4** with Metal Ions

UV titrations of **4** with Zn(OTf)₂, Eu(OTf)₃ were performed to check the complexation of **4** with metal ions. In a typical experiment, the ratio of ligand to metal was varied, while keeping the overall concentration of ligand constant (0.050 mmol/L).

1.5 UV Titration of Zn:**4** and Eu:**4** with Solvents

UV titrations of Zn:**4** and Eu:**4** with solvents were performed to check the effects of solvents on the stability of the complexes. In a typical experiment, the ratio of solvent to complex was varied, while keeping the overall concentration of complex constant (0.050 mmol/L).

1.6 Swelling Tests of Gels

The swelling tests were carried out to obtain the critical concentrations where the gels started to flow. Three systems were studied containing different stoichiometric ratios of Zn(II) to Eu(III) ranging

from 100% Zn(II) and no Eu(III) (100/0), to 50% Zn(II) and 50% Eu(III) (50/50), and to no Zn(II) and 100% Eu(III) (0/100). The study was conducted by adding various amounts of solvent in a stepwise manner into vials containing 50 mg supramolecular polymers, and checking the homogenization rate and gel stability by inverting the vials.

1.7 Optical Properties of Gels

To study the optical properties of the gels, photoluminescence spectra were measured for various systems (gels or sols of **Zn:5**, **Eu:5**, **Zn/Eu:5**) with varying amounts of Zn(II) or Eu(III) or a combination of Zn(II) and Eu(III). To acquire their photoluminescence spectra, gels were loaded into quartz cuvettes (1 cm optical length) and excited at 365 nm. Also, various gels were irradiated with 365 nm UV light and the images were taken by a digital camera.

1.8 Temperature Responsiveness of Gels

To test the temperature responsiveness of the gels, gels of 50 mg/mL in sealed vials were heated in oil bath and the gel stability was checked by inverting the vials. Also, the photoluminescence changes in the gels after being heated were checked by irradiating with 365 nm UV light.

1.9 Chemical Responsiveness of Gels

Chemicals including DMSO, DMF, CH₃OH, HCOOH, (EtO)₃PO, PPh₃, PMDETA, bipyridine (BPy) were selected to test the chemical responsiveness of the gels. The original concentrations of the gels were 50 mg/mL. For liquid chemicals, a total of 0.5 mL chemical was added. For solid chemicals, 0.5 g solid was dissolved with chloroform to make 0.5 mL solution before used. After addition of the chemicals, the gel stability was checked with or without shaking the vials. Pictures of the photoluminescence after homogenization of the chemicals were recorded. Also, for some chemicals, the evolution of photoluminescence during the homogenization was tracked.

1.10 Self-Healing of Coating

A supramolecular polymer **Eu:5** containing only 0.7 eq of Eu(III) (**0/70**) was used as a coating material for various metal surfaces. In this study, iron, copper and zinc plated iron were selected to provide different surfaces. Iron and copper were mechanically polished to give fresh surface. Before

applying supramolecular coating on the surfaces, the surfaces were cleaned with soap and rinsed with acetone, followed by drying with N₂ flow. Then solution of the supramolecular polymer **Eu:5** was casted on the surface and allowed to dry at RT and further dried in vacuo.

The preliminary examination on the adhesive strength of the coating on metal surface was conducted by pulling off the coating with a pair of tweezers.

II. Supplementary Results

2.1 NMR

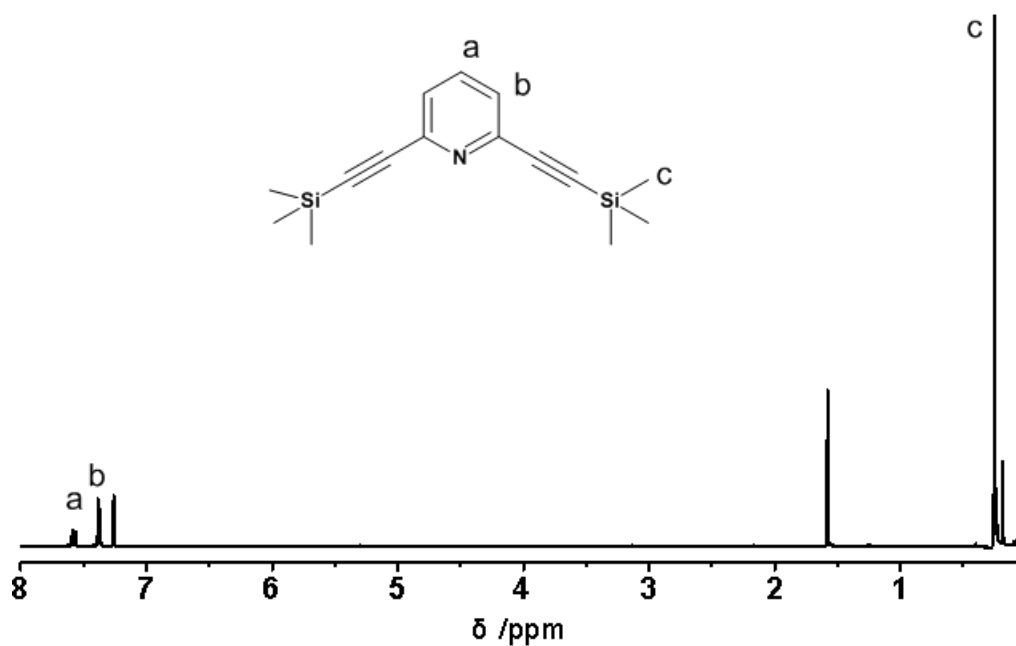


Figure S1. ¹H NMR of **1** in CDCl₃.

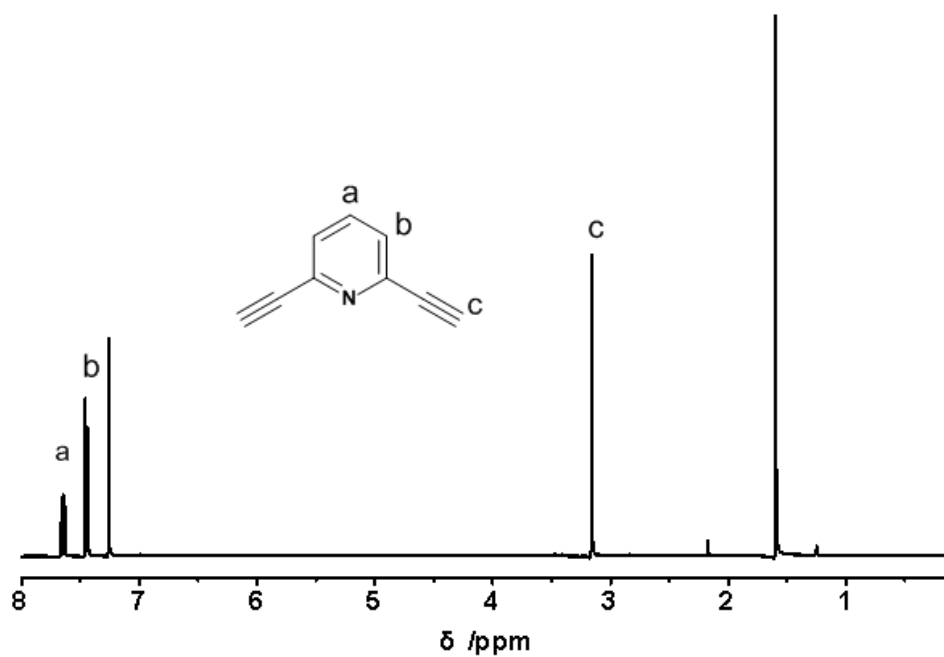


Figure S2. ^1H NMR of 2 in CDCl_3 .

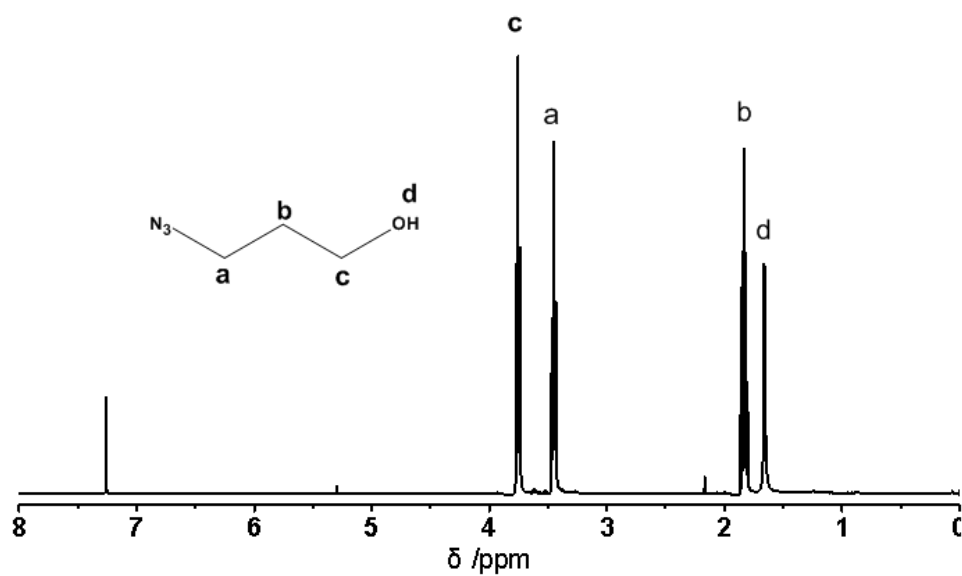


Figure S3. ^1H NMR of 3 in CDCl_3 .

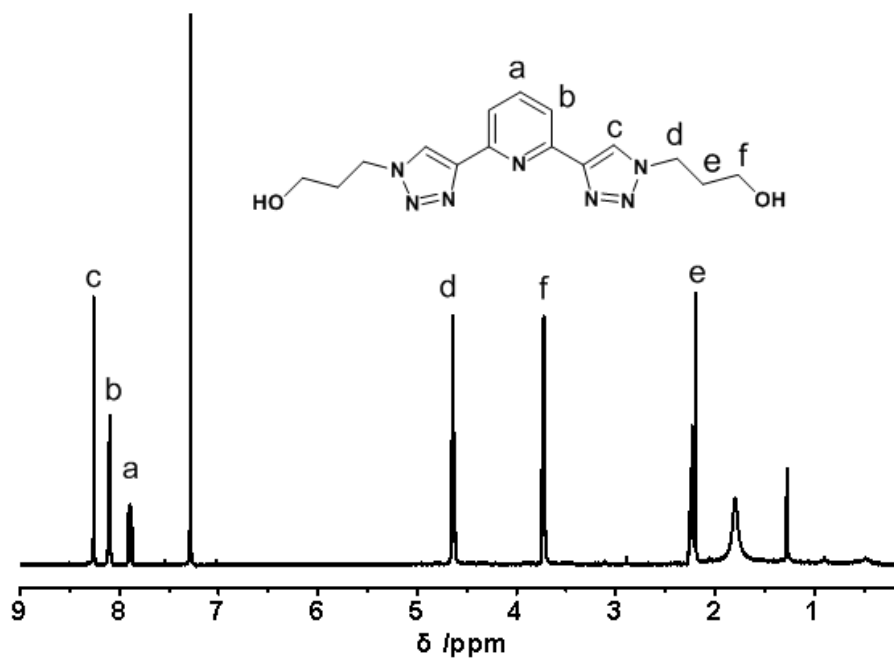


Figure S4. ¹H NMR of 4 in CDCl₃.

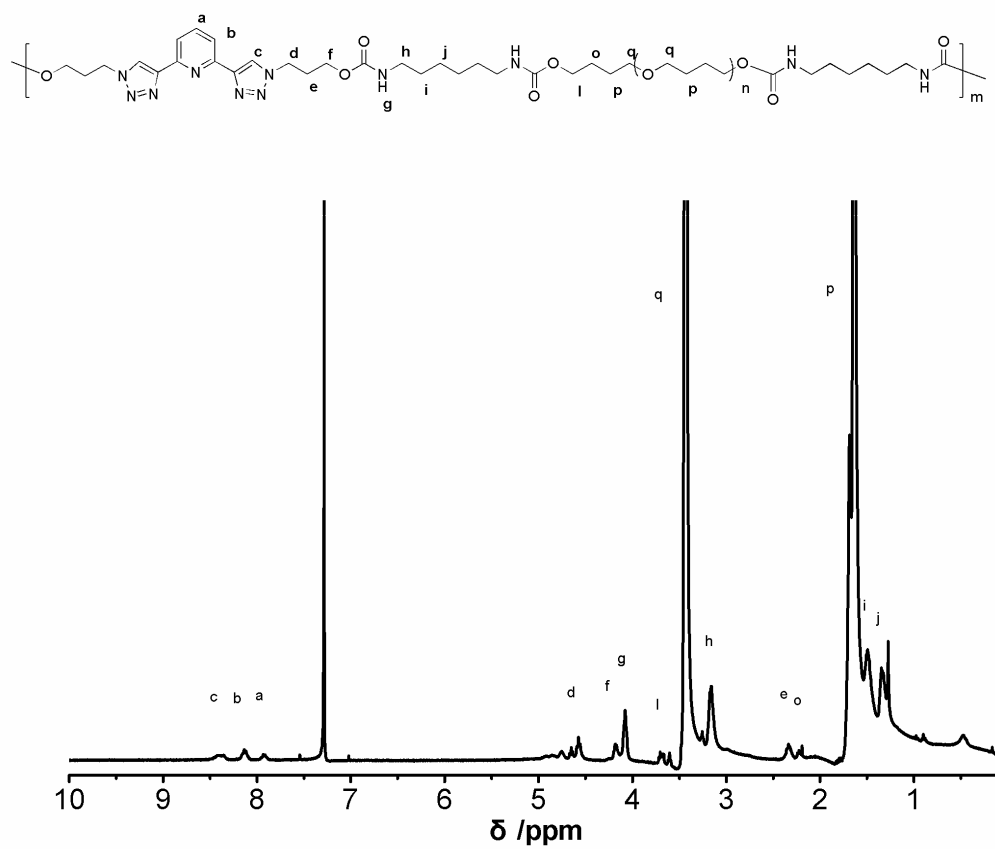


Figure S5. ¹H NMR of 5 in CDCl₃.

2.2 GPC

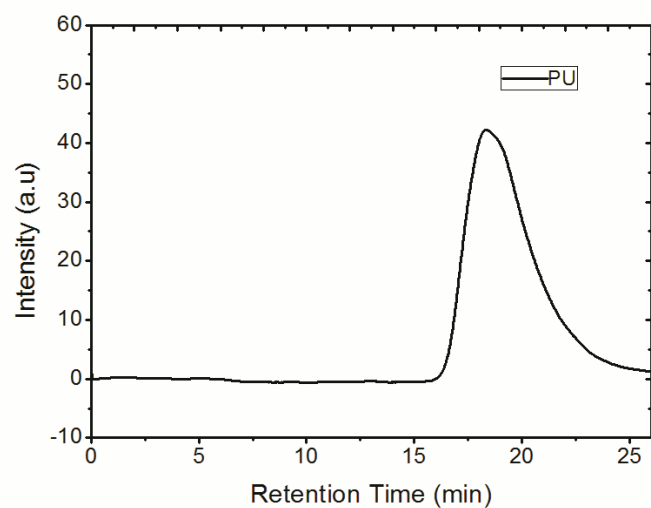


Figure S6. GPC trace of **5** in THF.

2.3 FTIR

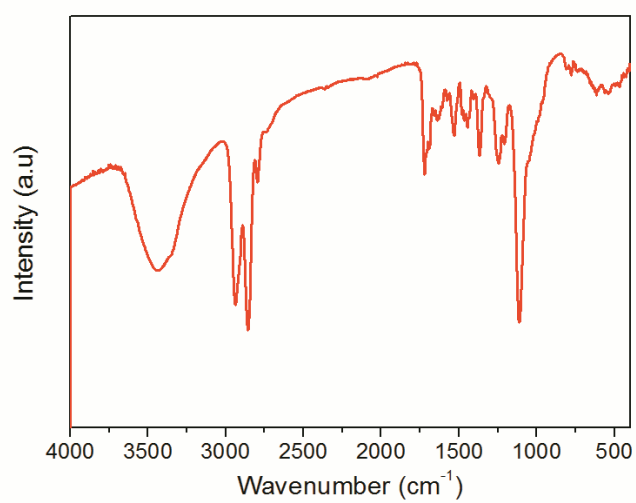


Figure S7. FTIR of **5**.

2.4 UV Titration of **4** with Metal Ions

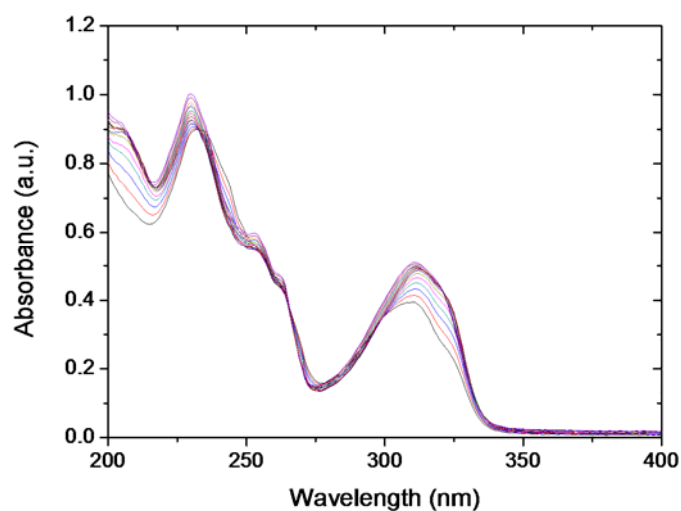


Figure S8. UV titration experiment of **4** (0.05 mM) with $\text{Zn}(\text{OTf})_2$ in acetonitrile.

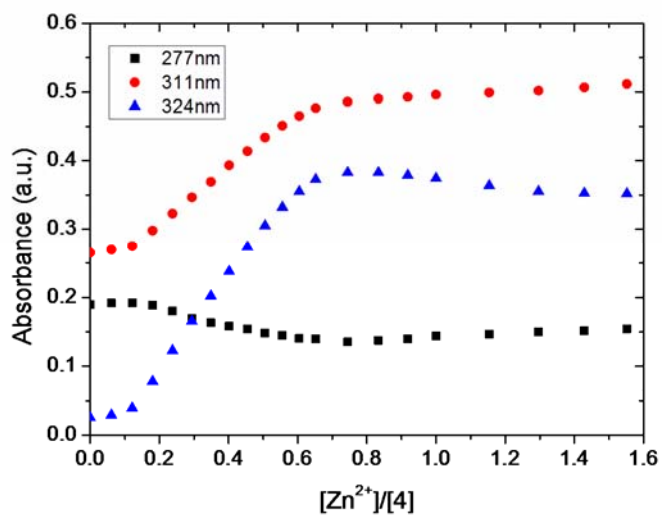


Figure S9. The absorption intensities at various wavelengths from Figure S8 are plotted as a function of metal to ligand ratio.

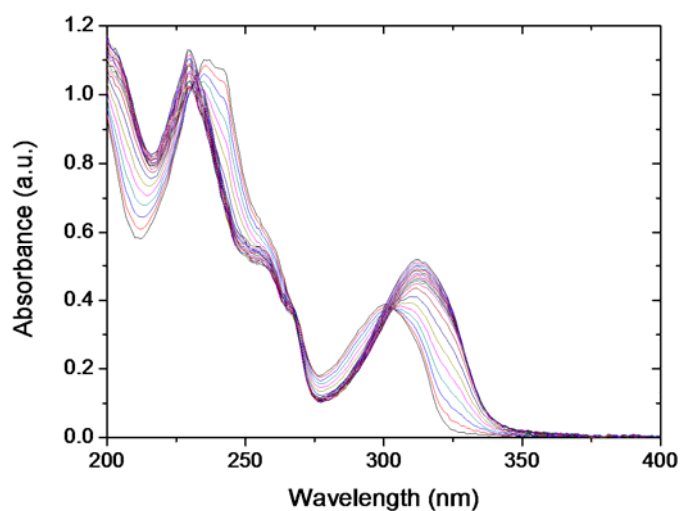


Figure S10. UV titration experiment of **4** (0.05 mM) with $\text{Eu}(\text{OTf})_3$ in acetonitrile.

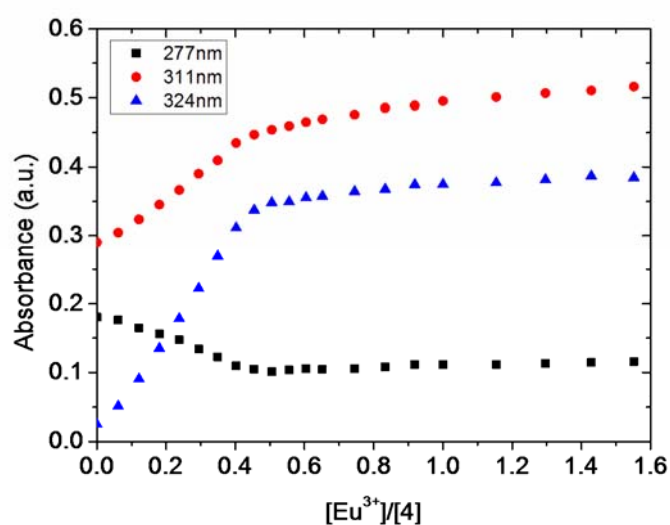


Figure S11. The absorption intensities at various wavelengths from Figure S10 are plotted as a function of metal to ligand ratio.

Note: As water has not been excluded during the titration experiment a reasonable explanation for the deviations from 1:2 for **Zn:4** and 1:3 for **Eu:4** might be the role of water as a competing ligand.

2.4 UV Titration of Zn:4 and Eu:4 with Solvents and Chemical

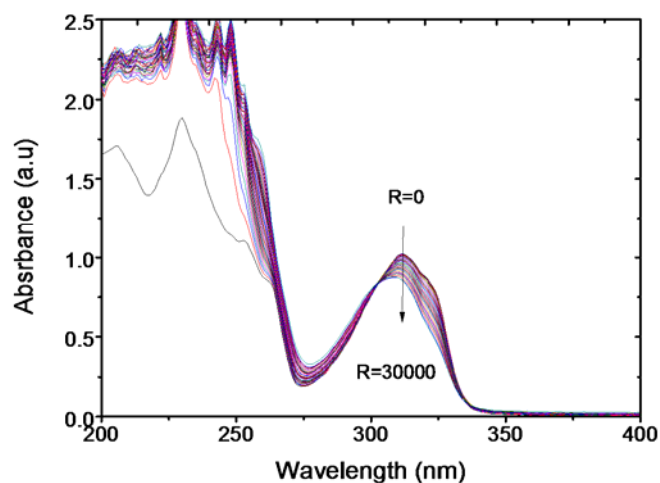


Figure S12. The UV spectral change upon titration of DMF solution into **Zn:4** at various values of $R = [\text{DMF}]/[\text{Zn}^{2+}]$.

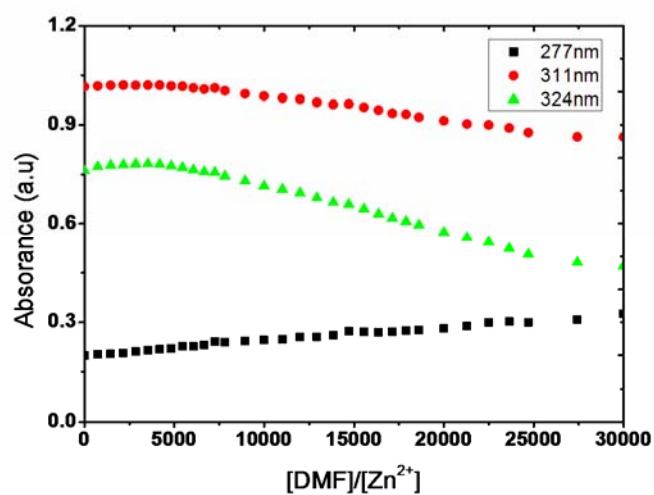


Figure S13. The absorbance changes plotted against the ratio $R = [\text{DMF}]/[\text{Zn}^{2+}]$ at various wavelengths from Figure S12.

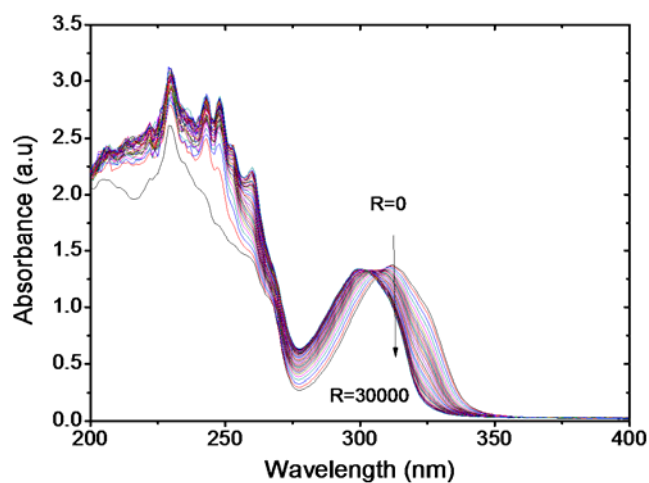


Figure S14. The UV spectral change upon titration of DMF solution into **Eu:4** at various values of $R = [\text{DMF}]/[\text{Eu}^{3+}]$.

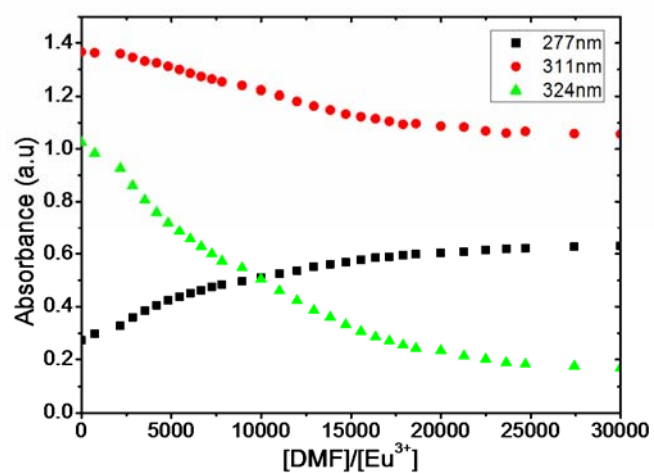


Figure S15. The absorbance changes plotted against the ratio $R = [\text{DMF}]/[\text{Eu}^{3+}]$ at various wavelengths from Figure S14.

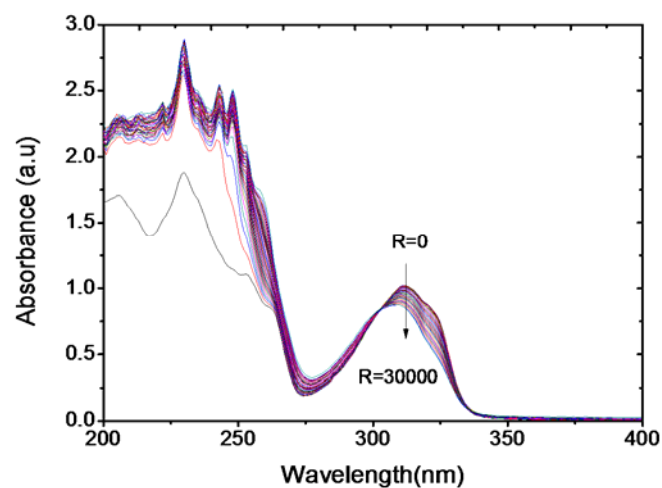


Figure S16. The UV spectral change upon titration of DMSO solution into **Zn:4** at various values of $R = [\text{DMSO}]/[\text{Zn}^{2+}]$.

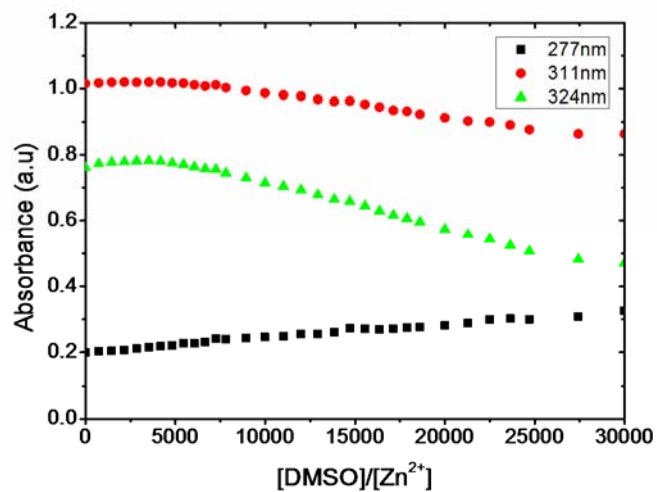


Figure S17. The absorbance changes plotted against the ratio $R = [\text{DMSO}]/[\text{Zn}^{2+}]$ at various wavelengths from Figure S16.

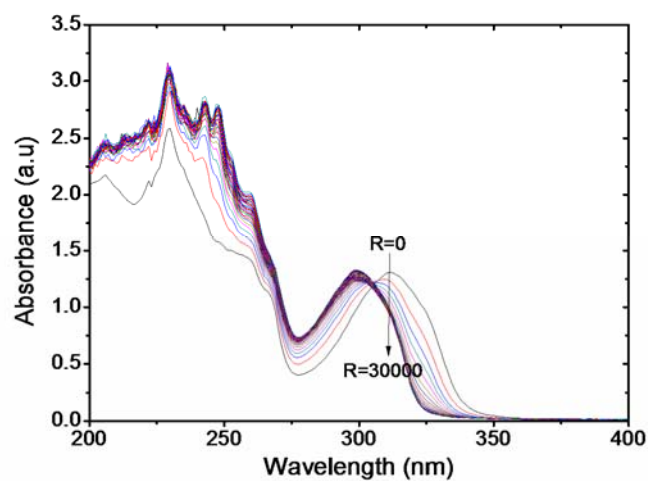


Figure S18. The UV spectral change upon titration of DMSO solution into **Eu:4** at various values of $R = [\text{DMFSO}]/[\text{Eu}^{3+}]$.

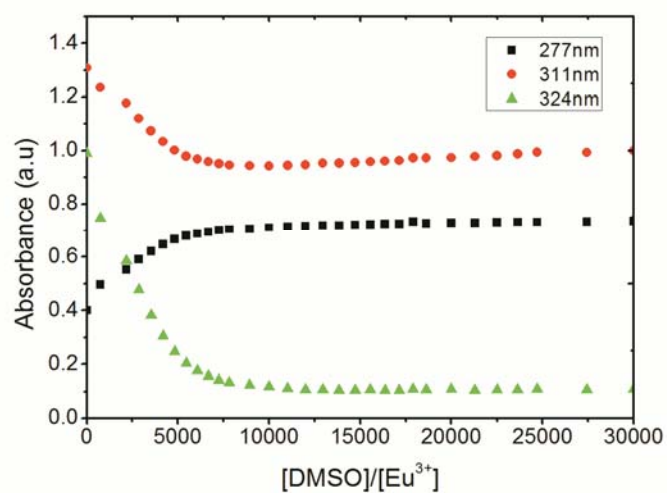


Figure S19. The absorbance changes plotted against the ratio $R = [\text{DMSO}]/[\text{Eu}^{3+}]$ at various wavelengths from Figure S18.

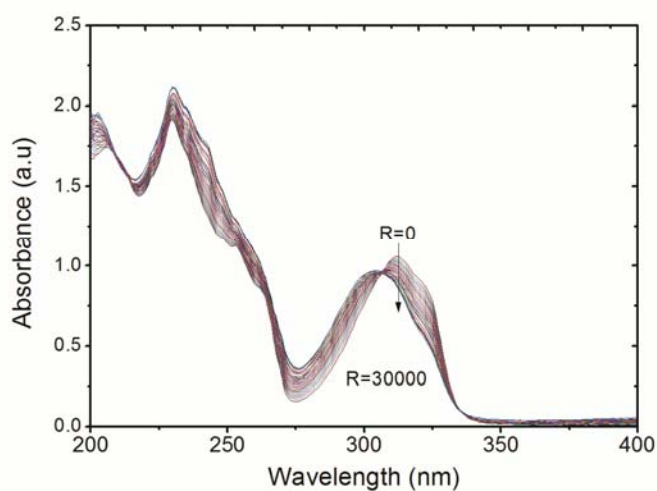


Figure S20. The UV spectral change upon titration of ethylene glycol (EG) solution into **Zn:4** at various values of $R = [\text{EG}]/[\text{Zn}^{2+}]$.

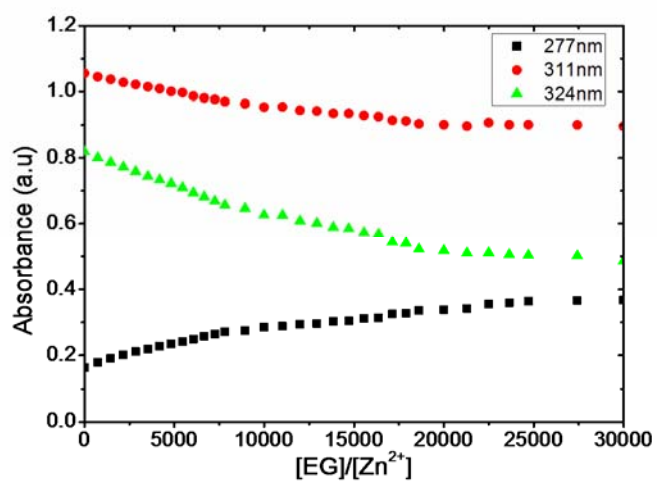


Figure S21. The absorbance changes plotted against the ratio $R = [\text{EG}]/[\text{Zn}^{2+}]$ at various wavelengths from Figure S20.

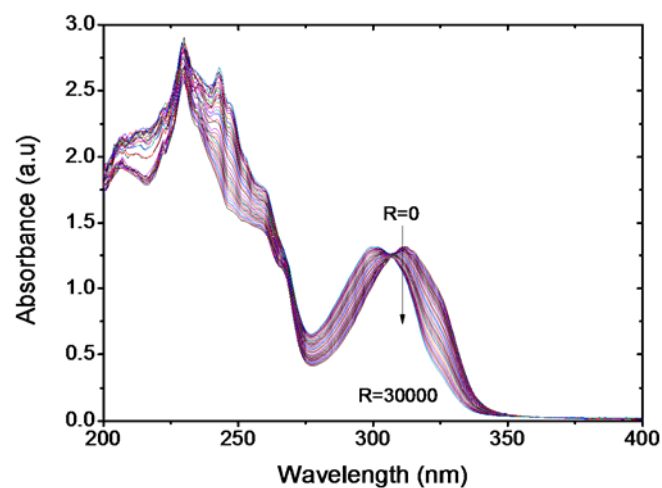


Figure S22. The UV spectral change upon titration of ethylene glycol (EG) solution into **Eu:4** at various values of $R = [\text{EG}]/[\text{Eu}^{3+}]$.

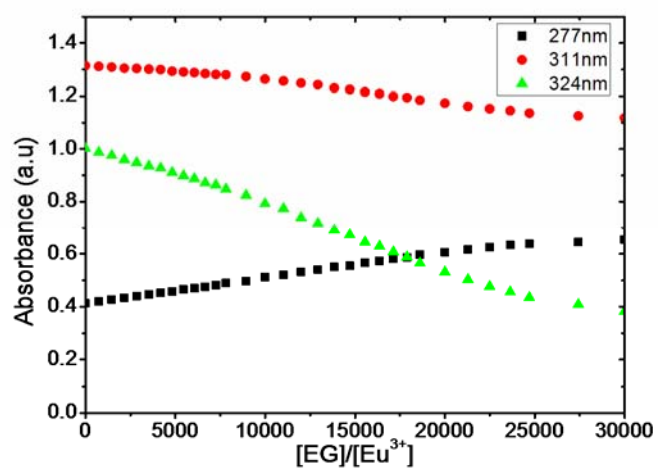


Figure S23. The absorbance changes plotted against the ratio $R = [\text{EG}]/[\text{Eu}^{3+}]$ at various wavelengths from Figure S22.

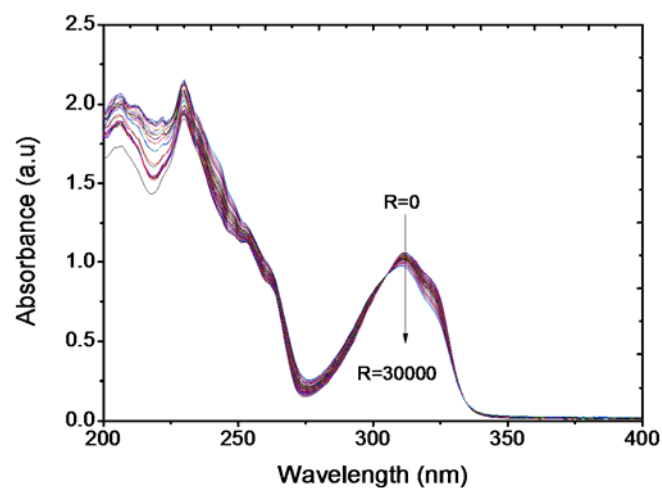


Figure S24. The UV spectral change upon titration of MeOH solution into **Zn:4** at various values of $R = [\text{MeOH}]/[\text{Zn}^{2+}]$.

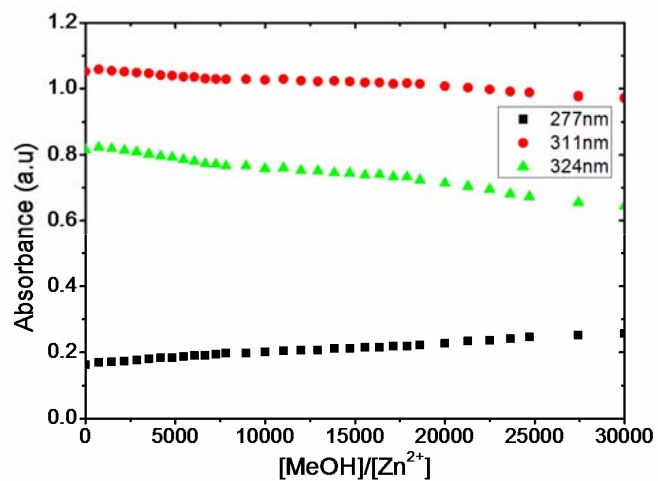


Figure S25. The absorbance changes plotted against the ratio $R = [\text{MeOH}]/[\text{Zn}^{2+}]$ at various wavelengths from Figure S24.

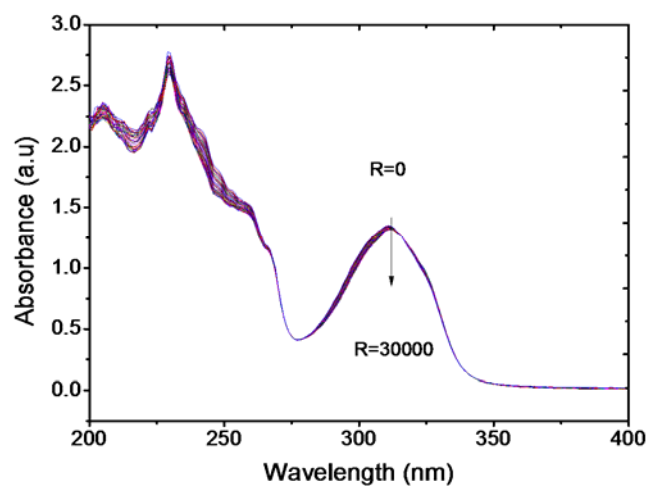


Figure S26. The UV spectral change upon titration of MeOH solution into **Eu:4** at various values of $R = [\text{MeOH}]/[\text{Eu}^{2+}]$.

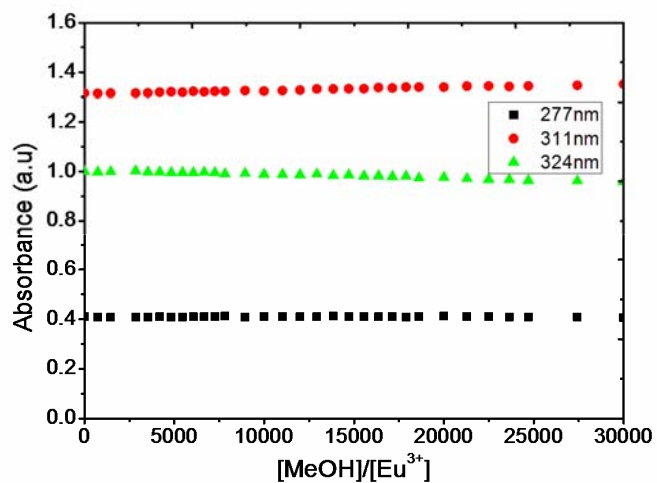


Figure S27. The absorbance changes plotted against the ratio $R = [\text{MeOH}]/[\text{Eu}^{3+}]$ at various wavelengths from Figure S26.

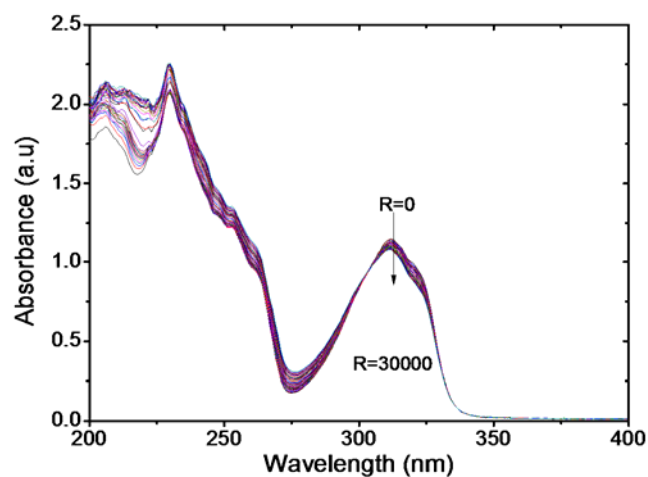


Figure S28. The UV spectral change upon titration of THF solution into **Zn:4** at various values of $R = [\text{THF}]/[\text{Zn}^{2+}]$.

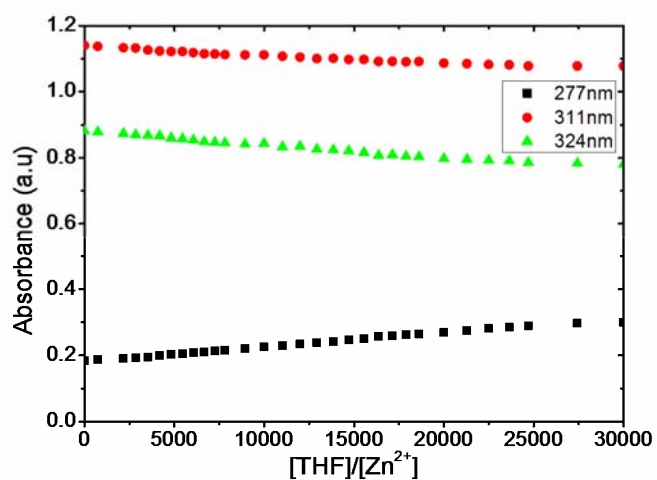


Figure S29. The absorbance changes plotted against the ratio $R = [\text{THF}]/[\text{Zn}^{2+}]$ at various wavelengths from Figure S28.

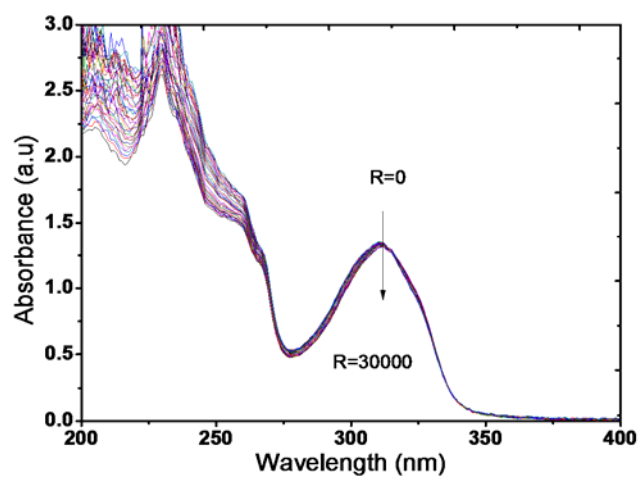


Figure S30. The UV spectral change upon titration of THF solution into **Eu:4** at various values of $R = [\text{THF}]/[\text{Eu}^{3+}]$.

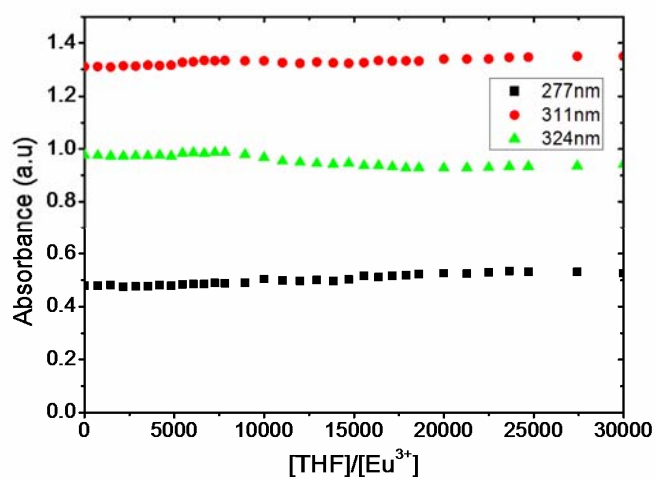


Figure S31. The absorbance changes plotted against the ratio $R = [\text{THF}]/[\text{Eu}^{3+}]$ at various wavelengths from Figure S30.

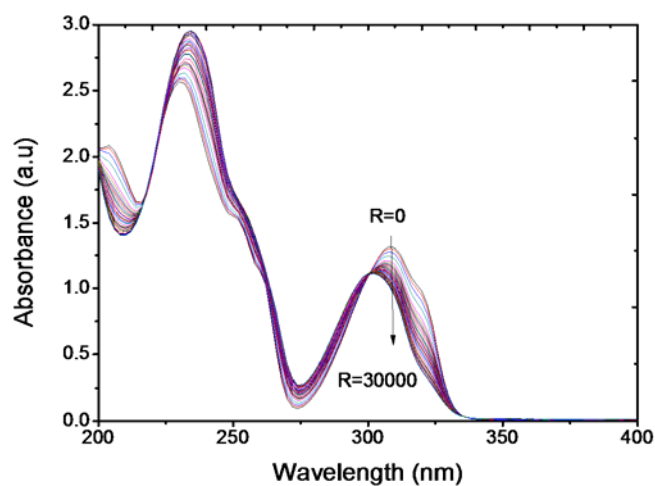


Figure S32. The UV spectral change upon titration of H₂O solution into **Zn:4** at various values of $R = [\text{H}_2\text{O}]/[\text{Zn}^{2+}]$.

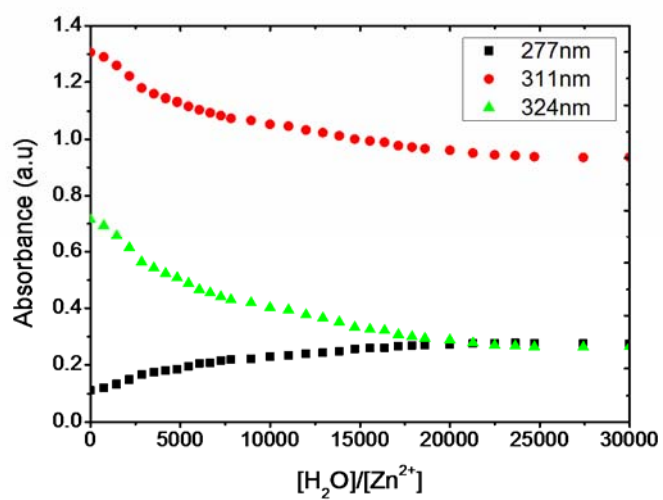


Figure S33. The absorbance changes plotted against the ratio $R = [\text{H}_2\text{O}]/[\text{Zn}^{2+}]$ at various wavelengths from Figure S32.

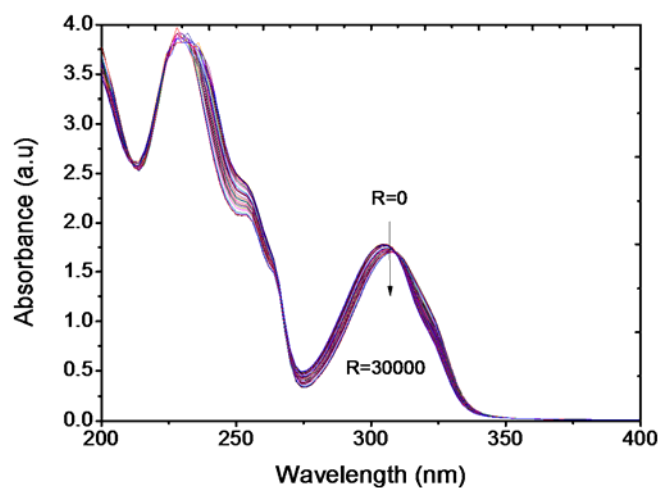


Figure S34. The UV spectral change upon titration of H₂O solution into **Eu:4** at various values of $R = [\text{H}_2\text{O}]/[\text{Eu}^{3+}]$.

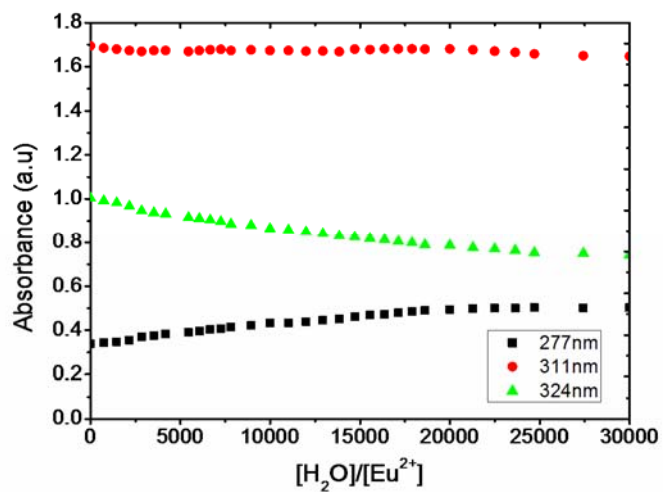


Figure S35. The absorbance changes plotted against the ratio $R = [\text{H}_2\text{O}]/[\text{Eu}^{3+}]$ at various wavelengths from Figure S34.

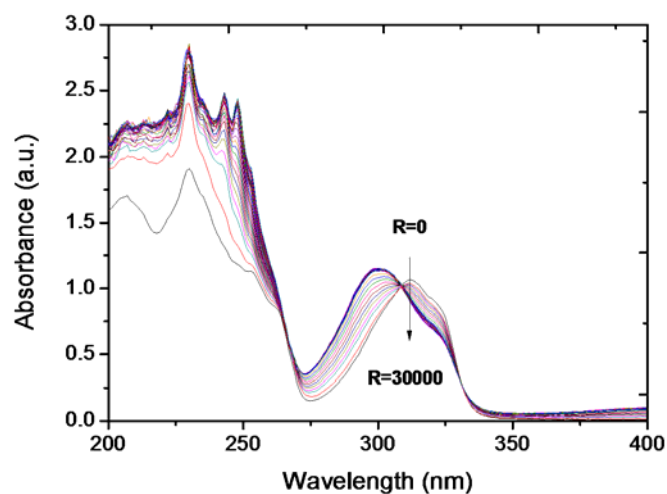


Figure S36. The UV spectral change upon titration of HCOOH solution into Zn:4 at various values of $R = [\text{HCOOH}]/[\text{Zn}^{2+}]$.

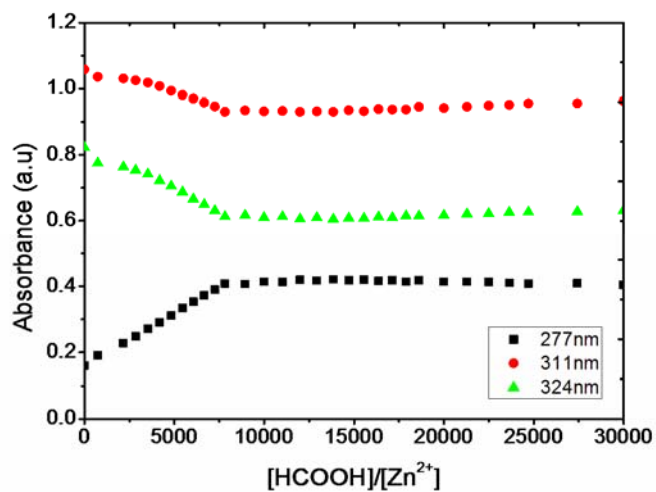


Figure S37. The absorbance changes plotted against the ratio $R = [\text{HCOOH}]/[\text{Zn}^{2+}]$ at various wavelengths from Figure S36.

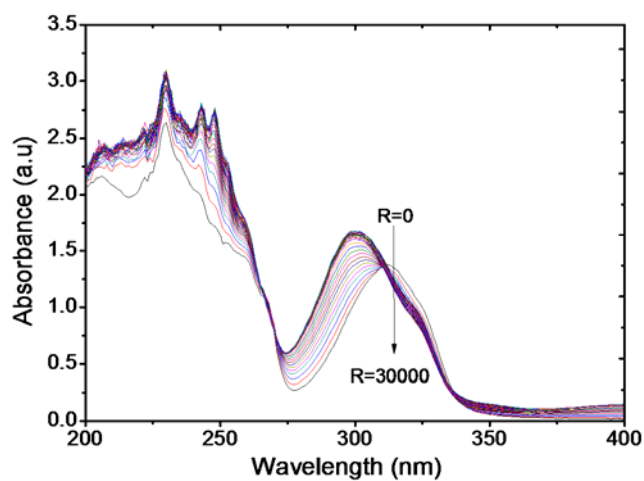


Figure S38. The UV spectral change upon titration of HCOOH solution into **Eu:4** at various values of $R = [\text{HCOOH}]/[\text{Eu}^{2+}]$.

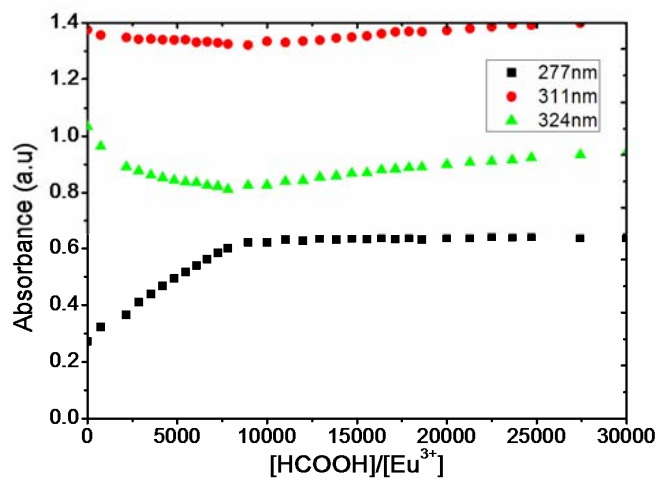


Figure S39. The absorbance changes plotted against the ratio $R = [\text{HCOOH}]/[\text{Eu}^{3+}]$ at various wavelengths from Figure S38.

2.5 Gelation

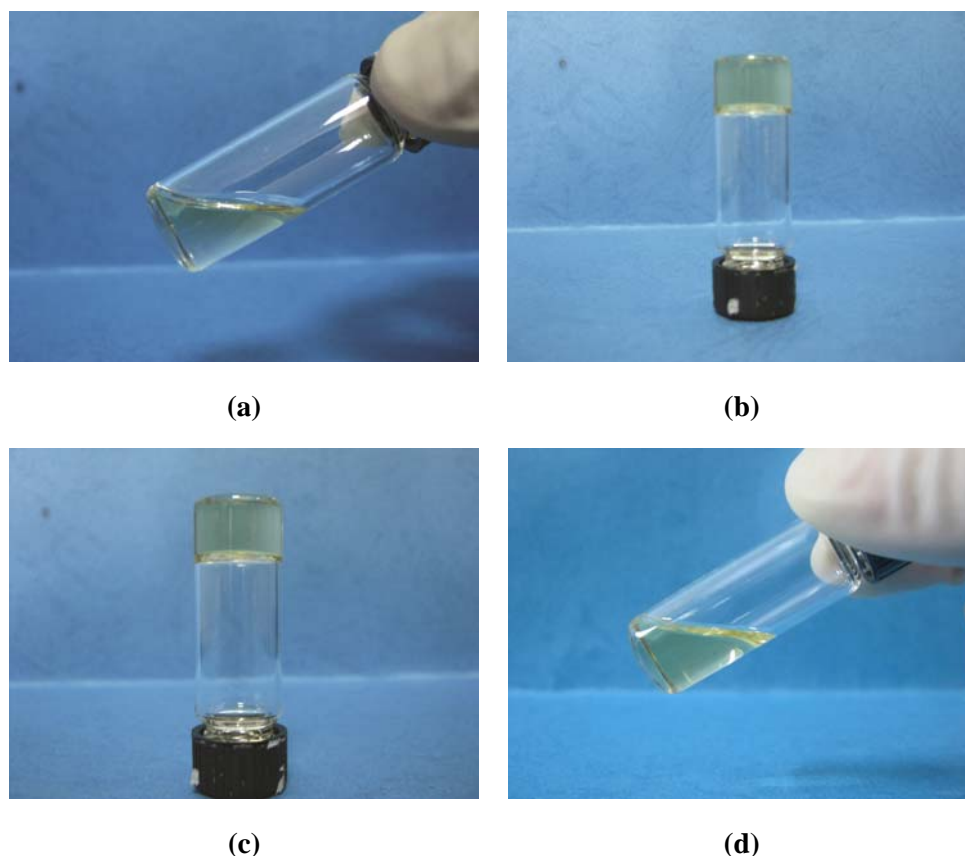


Figure S40. (a) Solution of **5** in CHCl_3 (100 mg/mL) before adding metal ions; (b) gel formed after addition of stoichiometric amount of $\text{Zn}(\text{OTf})_2$ dissolved in CH_3CN (0.05 mmol/mL); (c) gel formed after addition of stoichiometric amount of $\text{Zn}(\text{OTf})_2$ dissolved in THF (0.05 mmol/mL); (d) no gel formed after addition of stoichiometric amount of $\text{Zn}(\text{OTf})_2$ dissolved in MeOH (0.05 mmol/mL).

The first solution of **5** had a concentration of 100 mg/mL (100 mg **5** dissolved in 1 mL CHCl_3). In the cases of acetonitrile and THF, upon progressive addition of solutions of metal salts, gradual increase in viscosity was firstly observed, then at some point (about 50% and 35% of the stoichiometric amounts for Zn(II) and Eu(III) added, respectively) gels were formed. The difference in the amounts of Zn(II) and Eu(III) required to reach the gel points is consistent with their different binding characteristics, i.e. Zn(II) binds to BTP in a 1:2 ratio and Eu(III) binds in a 1:3 ratio. When methanol was used as the solvent to dissolve the metal salts, however, no gels can be formed, despite that a slight increase in viscosity was observed. This difference in gelation should be due to the strong chelating ability of methanol which prevented the formation of stable or long-lived metal-BTP complexes. When a second solution of **5** having a concentration of 25 mg/mL was used, however, no

gelation was observed whichever solvent was used to prepare the solutions of metal salts. Since the second solution of **5** had a concentration only 1/4 of the first one, it is assumed that at this dilute condition the tendency to form intrachain loops would be higher than at concentrated conditions. In addition, acetonitrile, THF and methanol are coordinating by nature, their presence will influence the lifetimes of metal-ligand complexes. Nevertheless, upon condensation and equilibration, gels could be eventually obtained for the systems in which acetonitrile and THF were used to prepare metal ion solutions. It is also noteworthy that after solvent evaporation the resulting materials from all the above mentioned different approaches could be re-swollen by appropriate solvents to form gels.

2.6 Swelling of Gels

In each case, a piece of dried gel of 50 mg was used. Swelling study was performed by means of stepwise addition of chloroform and checking the stability of the gels by inverting the vials after equilibration at each step. The equilibration time, defined as the time required for the absorption of solvent and the following homogenization of the gels, was different for different systems. It took about 30 min for the system containing only Zn(II) and about 3 min for the one containing only Eu(III), while the time required for the one containing 50% Zn(II) and 50% Eu(III) lied in between 3-30 min. The observation that longer equilibration times were required for the Zn(II) containing systems can be explained by the fact that Zn(II) forms stronger and less dynamic complex with BTP than does Eu(III). It should be pointed out that if different amounts of dried gels were used, the equilibration times might be different. Based on the inverting vial method, the critical concentrations for the gels to stay stable (no flowing) were about 20 mg/mL, 16.7 mg/mL and 14.3 mg/mL for the three systems, respectively, with the only Zn(II) one having the highest concentration and the only Eu(III) one having the lowest concentration (Supporting Information). Further addition of chloroform eventually led to complete dissolution of the gels. Similarly, all gels could be recovered by drying and reswelling. It is generally believed that higher crosslinking leads to lower swelling ratio. However, the Eu(III) containing systems, which are supposed to be more crosslinked, exhibited lower critical gel concentrations. A plausible explanation for this observation is that at similar concentrations the systems containing more Zn(II) were weaker in mechanical strength and therefore tended to flow at higher critical concentrations, although crosslinked networks still remained at this point.

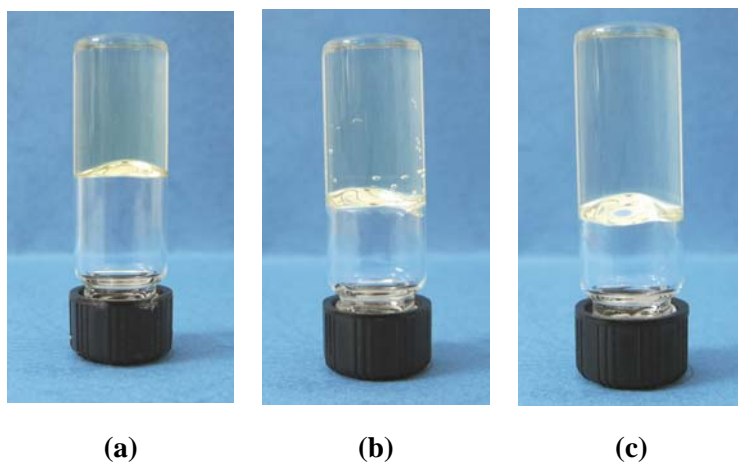


Figure S41. Swelling of gels with varying amounts of Zn(II) and Eu(III): (a) 100/0, (b) 50/50, (c) 0/100. Images shown are the gels at maximum swelling ratio (mL/g): (a) 50, (b) 60 and (c) 70.

2.7 Rheological Behaviors

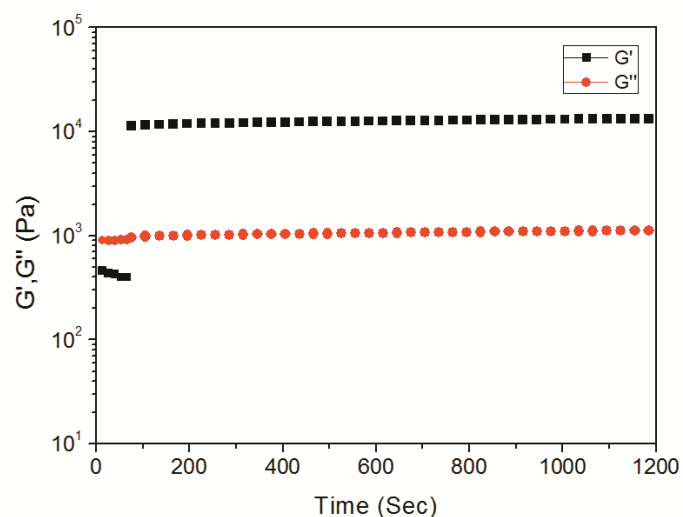


Figure S42. Recovery behaviour of a gel (60 mg/mL) containing only Eu(III) after preshear.

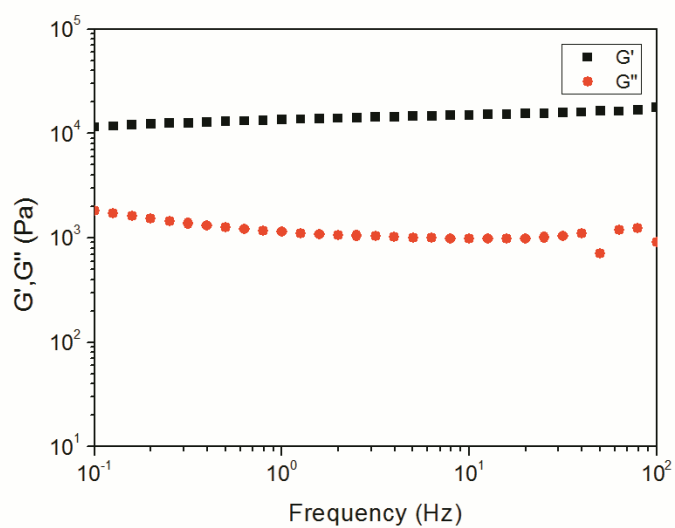


Figure S43. Frequency sweep of a gel (60 mg/mL) containing only Eu(III) after equilibration.

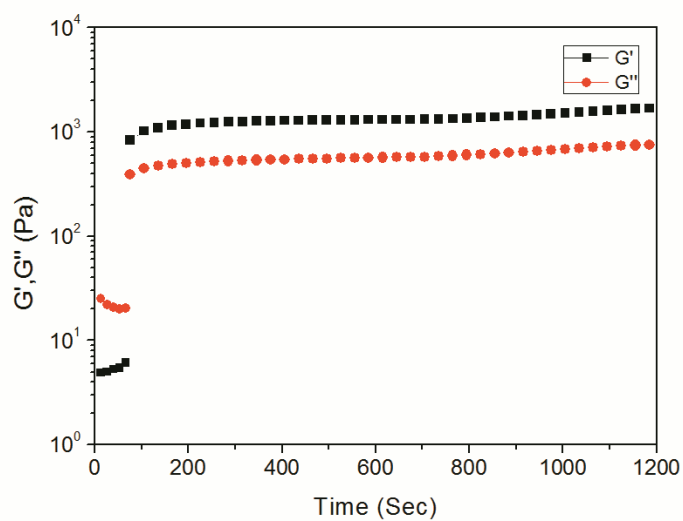


Figure S44. Recovery behaviour of a gel (45 mg/mL) containing only Zn(II) after preshear.

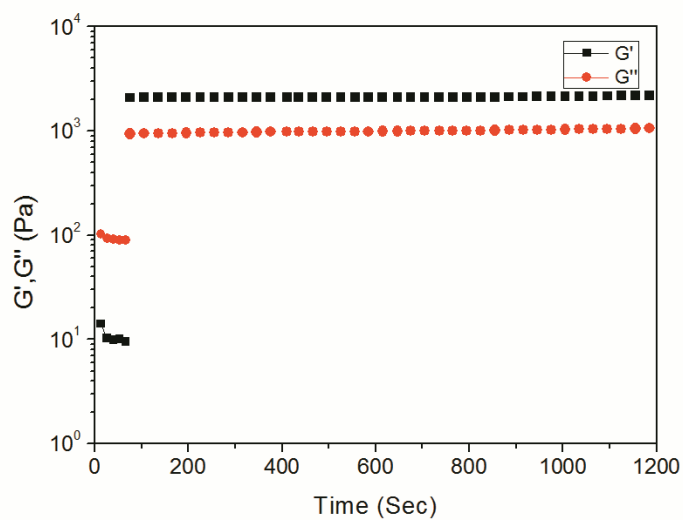


Figure S45. Recovery behaviour of a gel (60 mg/mL) containing only Zn(II) after preshear.

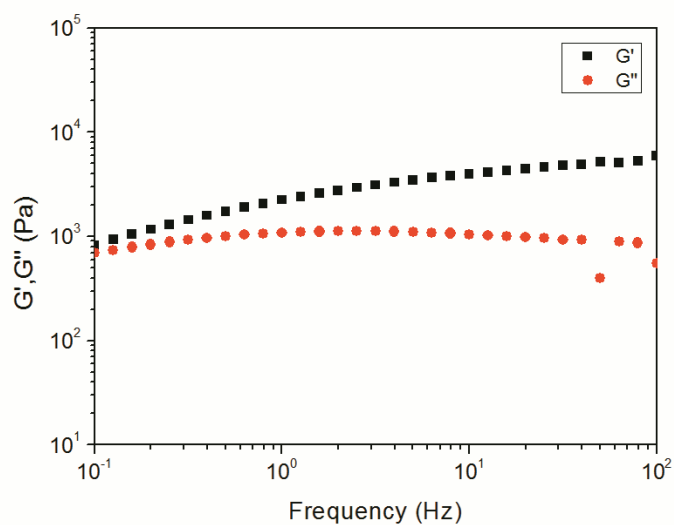


Figure S46. Frequency sweep of a gel (60 mg/mL) containing only Zn(II) after equilibration.

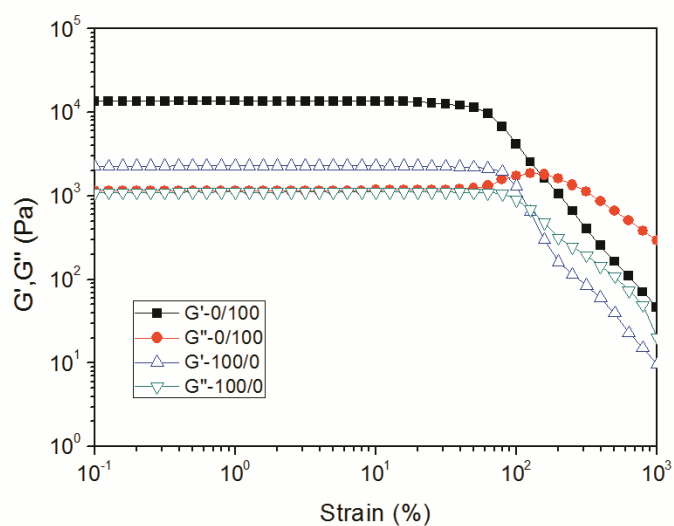


Figure S47. Strain sweeps of gel (60 mg/mL) containing only Zn(II) (**100/0**) and only Eu(III) (**0/100**) after equilibration.

2.8 Optical Properties

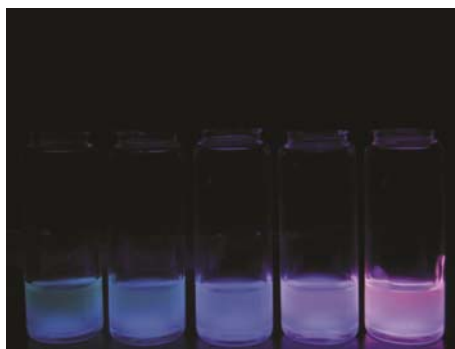


Figure S48. Picture of gels with varying amounts of Zn(II) and Eu(III) (from left to right Zn/Eu: 100/0, 75/25, 50/50, 25/75, 0/100) under 365 nm UV light demonstrating the effect of metal combination on the photoluminescence colour. Samples of 20 mg/mL were swollen by 1,1,2,2-tetrachloroethane.

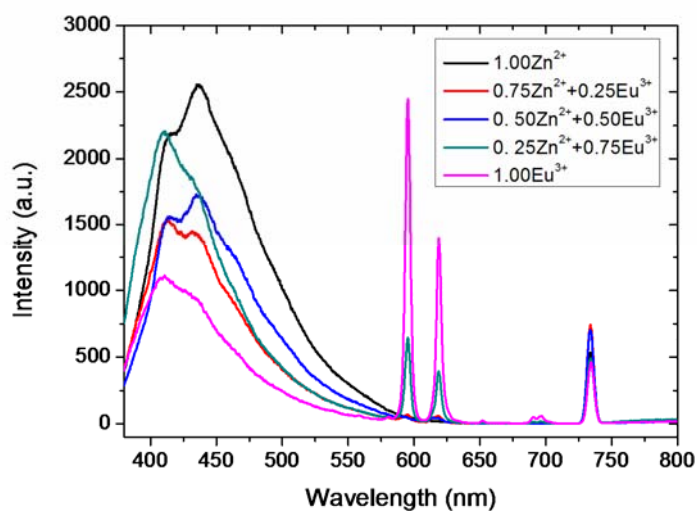


Figure S49. Photoluminescence spectra of Zn:5/Eu supramolecular gels with varying amounts of Zn(II) and Eu(III). Samples of 20 mg/mL were swollen or dissolved by CHCl₃.

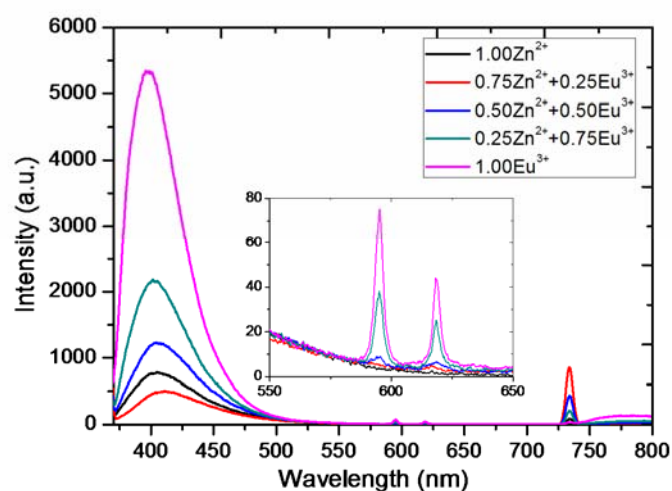


Figure S50. Photoluminescence spectra of **Zn:5/Eu** supramolecular gels with varying amounts of Zn(II) and Eu(III). Samples of 20 mg/mL were swollen or dissolved by 1,1,2,2-tetrachloroethane.

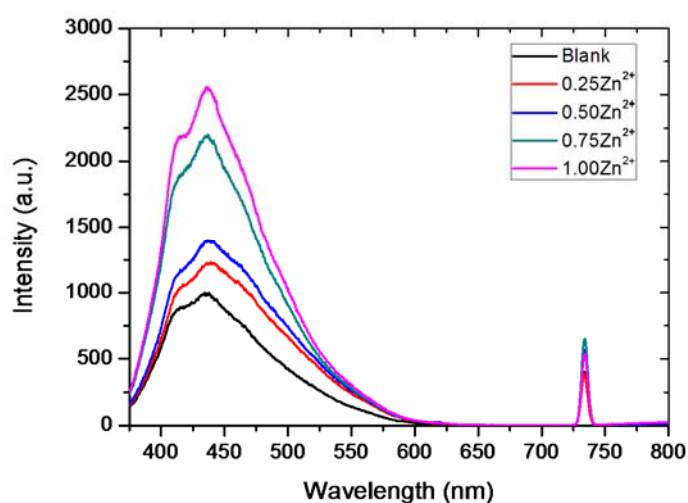


Figure S51. Photoluminescence spectra of **Zn:5** supramolecular polymers with varying amounts of Zn(II). Samples of 20 mg/mL were swollen or dissolved by CHCl₃.

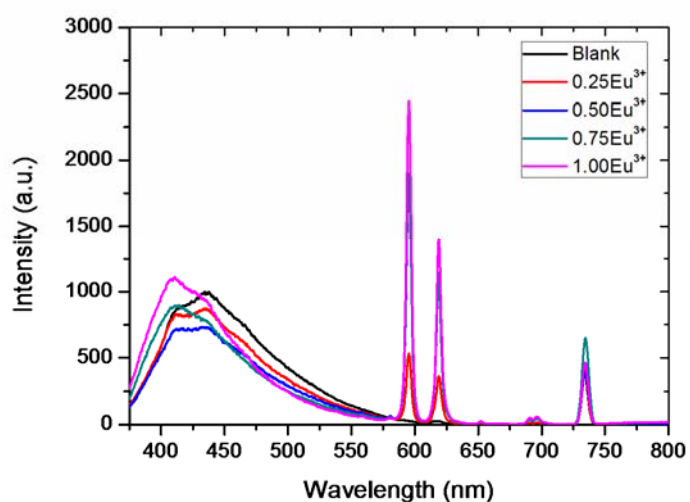


Figure S52. Photoluminescence spectra of **Eu:5** supramolecular polymers with varying amounts of **Eu(III)**. Samples of 20 mg/mL were swollen or dissolved by CHCl_3 .

2.9 Temperature Responsiveness

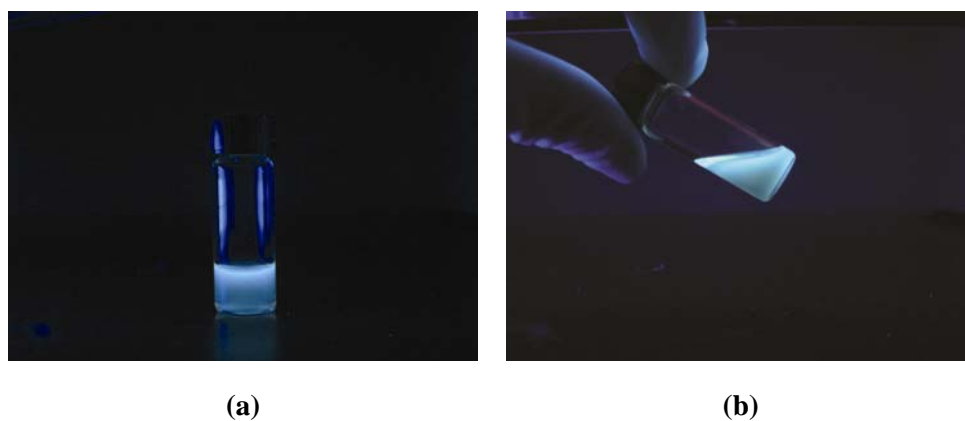


Figure S53. Pictures of a solution of pure **5** in CHCl_3 (20 mg/mL) under 365 nm UV light: (a) at RT, (b) after being heated at 140 °C.

2.10 Chemical Responsiveness

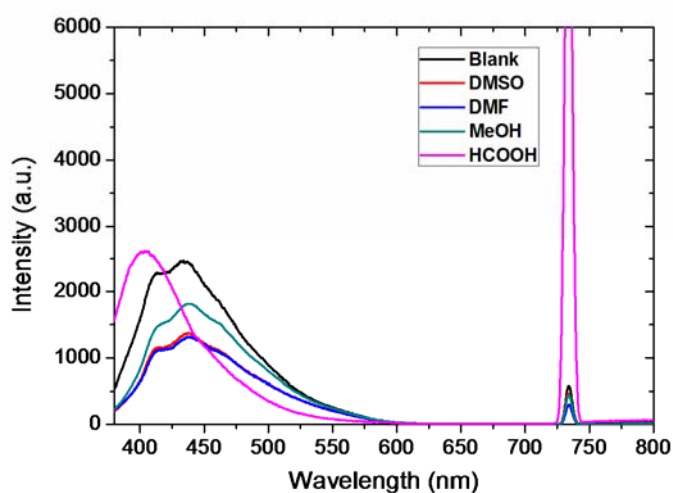


Figure S54. Photoluminescence spectra of supramolecular gels containing 100% Zn(II) before and after addition of various coordinating solvents and organic acid. The original gels of 50 mg/mL were swollen by CHCl_3 .

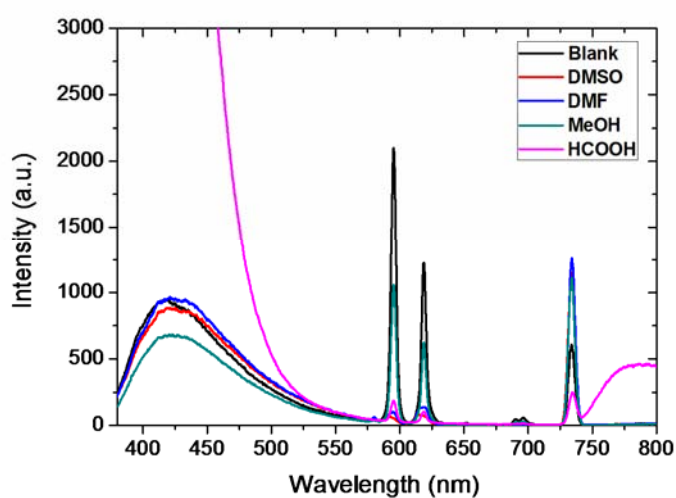


Figure S55. Photoluminescence spectra of supramolecular gels containing 100% Eu(III) before and after addition of various coordinating solvents and organic acid. The original gels of 50 mg/mL were swollen by CHCl_3 .

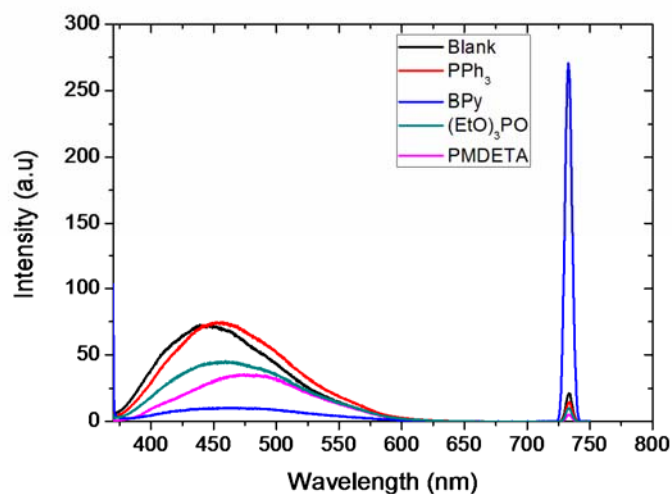


Figure S56. Photoluminescence spectra of supramolecular gels containing 100% Zn(II) before and after addition of various competing ligands. The original gels of 50 mg/mL were swollen by CHCl₃.

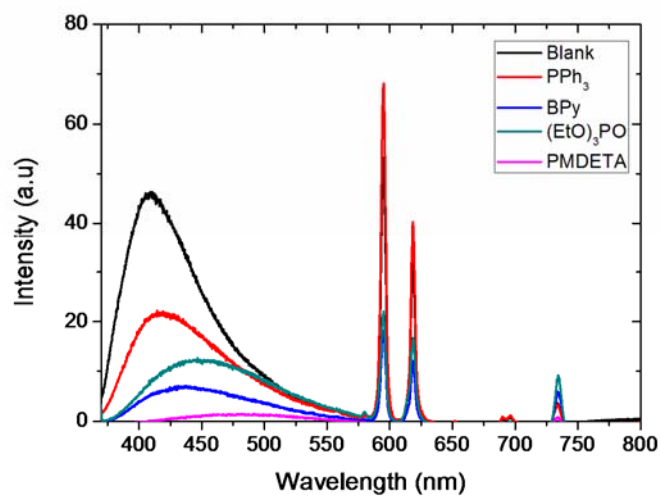
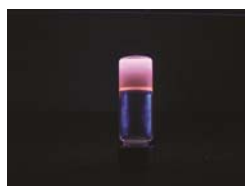
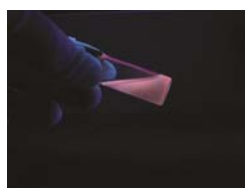
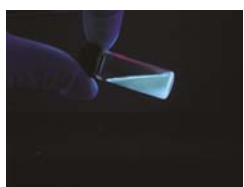
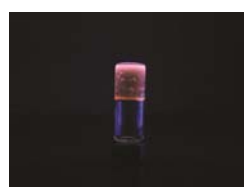


Figure S57. Photoluminescence spectra of supramolecular gels containing 100% Eu(III) before and after addition of various competing ligands. The original gels of 50 mg/mL were swollen by CHCl₃.

Table S1. Chemo-responsiveness of gels to various chemicals.

	100% Zn(II)		100% Eu(III)	
	$n_{\text{chem}}/n_{\text{metal}}^{[a]}$	Effect	$n_{\text{chem}}/n_{\text{metal}}^{[a]}$	Effect

None	N/A		N/A	
HCOOH	1328		2005	
(EtO)₃PO	334		505	
PMDETA	274		413	
BPy	365		551	
PPh₃	217		328	

[a] $n_{\text{chem}}/n_{\text{metal}}$ is the ratio of the amount of chemical added to the amount of metal ion in the gel.

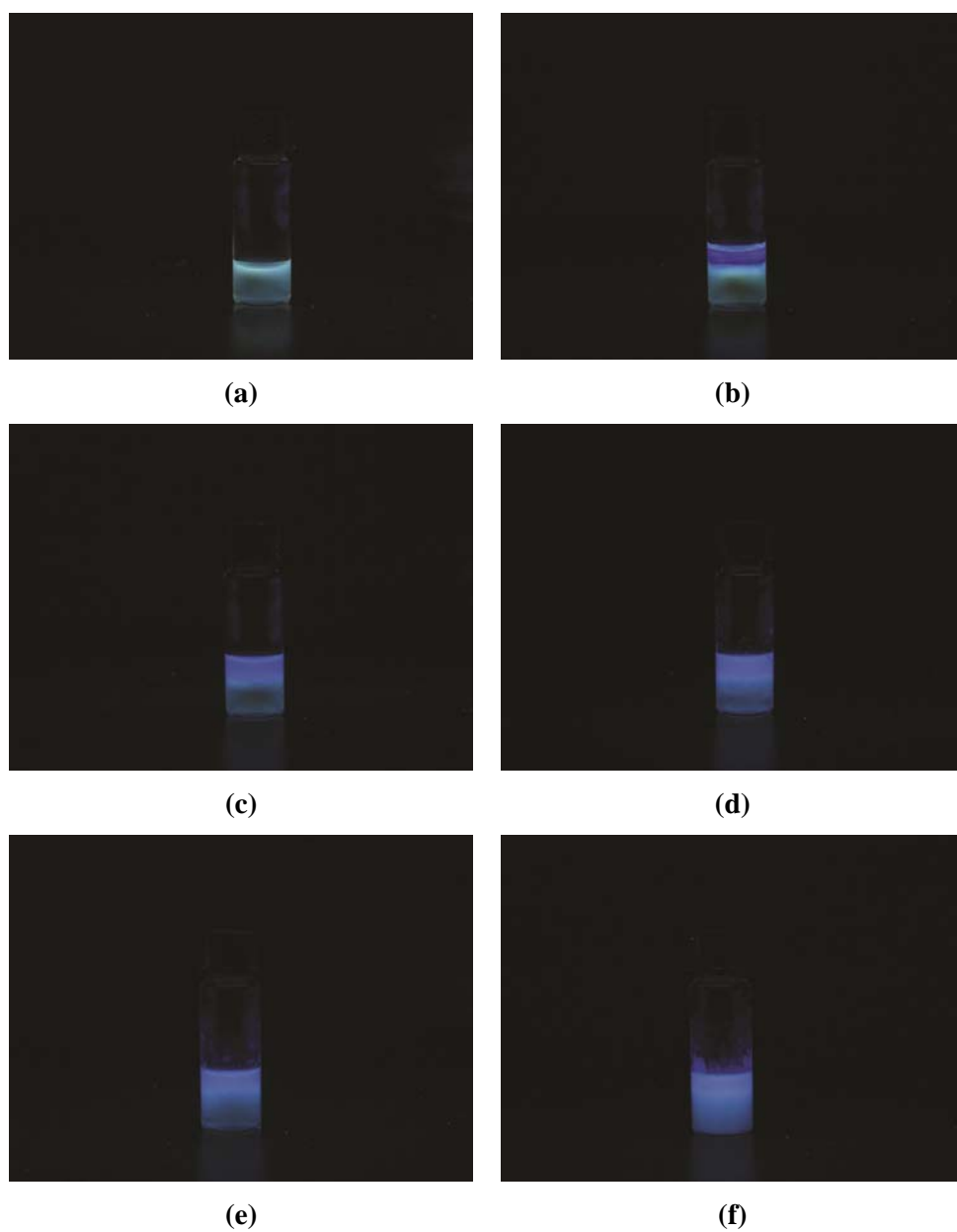


Figure S58. The evolution of photoluminescence of gel containing only Zn(II) upon addition of HCOOH on the top of the gel. (a) Original, and (b) 0 h, (c) 1 h, (d) 2 h, (e) 3 h, (f) 4 h after addition of HCOOH.

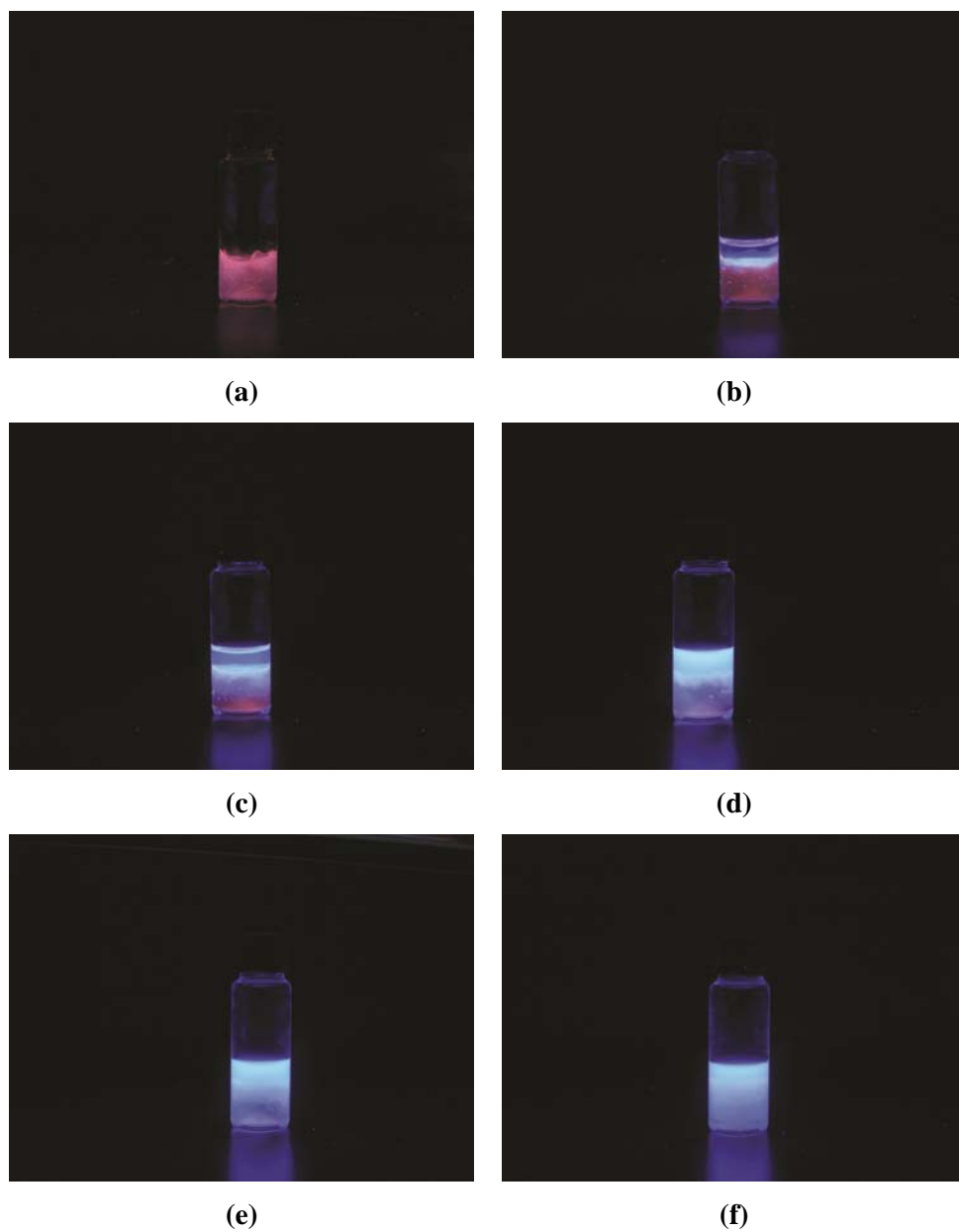


Figure S59. The evolution of photoluminescence of gel containing only Eu(III) upon addition of HCOOH on the top of the gel. (a) Original, and (b) 0 min, (c) 1 h, (d) 2 h, (e) 3 h, (f) 4 h after addition of HCOOH.

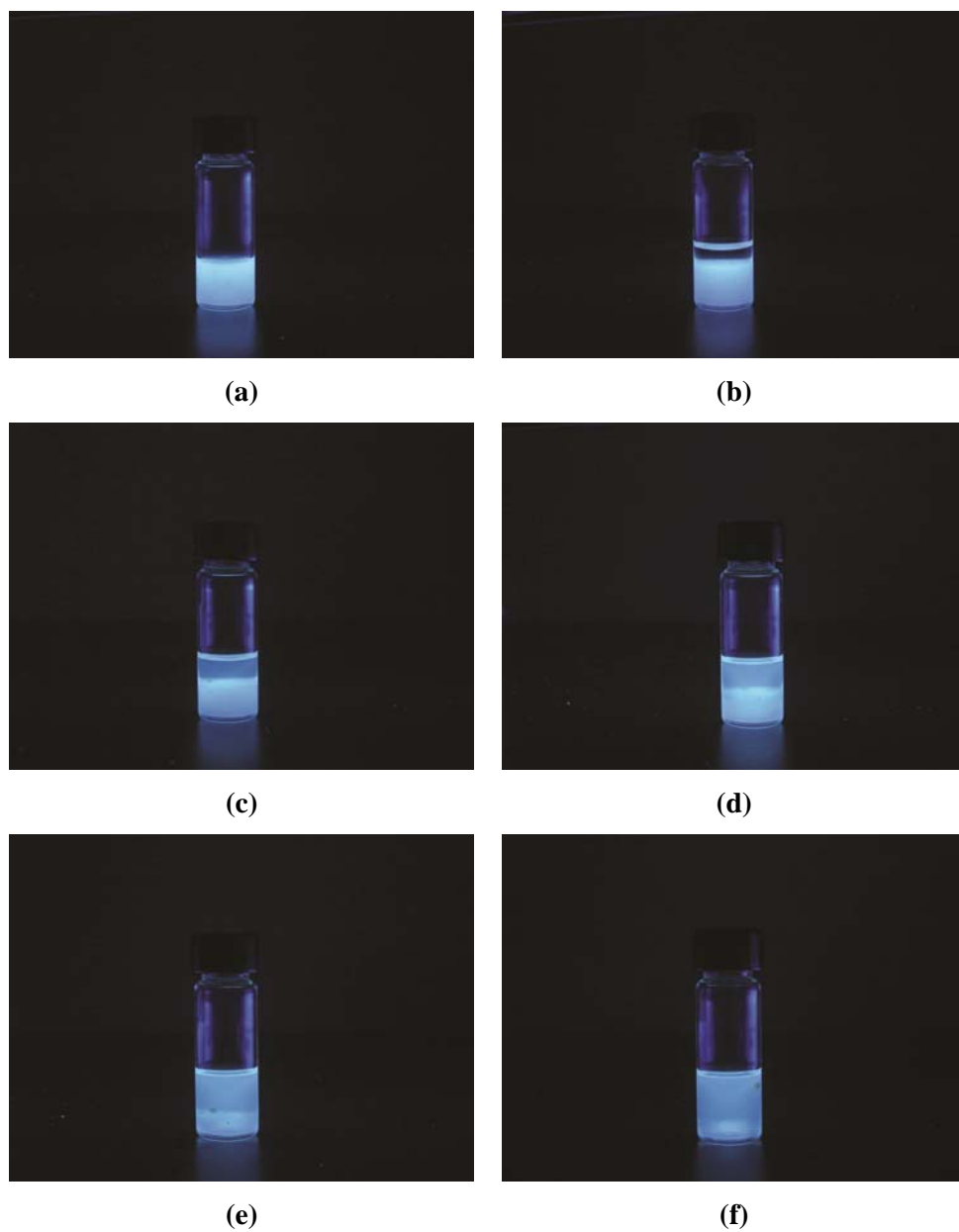


Figure S60. The evolution of photoluminescence of gel containing only Zn(II) upon addition of (EtO)₃PO on the top of the gel. (a) Original, and (b) 0 min, (c) 30 min, (d) 60 min, (e) 1.5 h, (f) 2 h after addition of (EtO)₃PO.

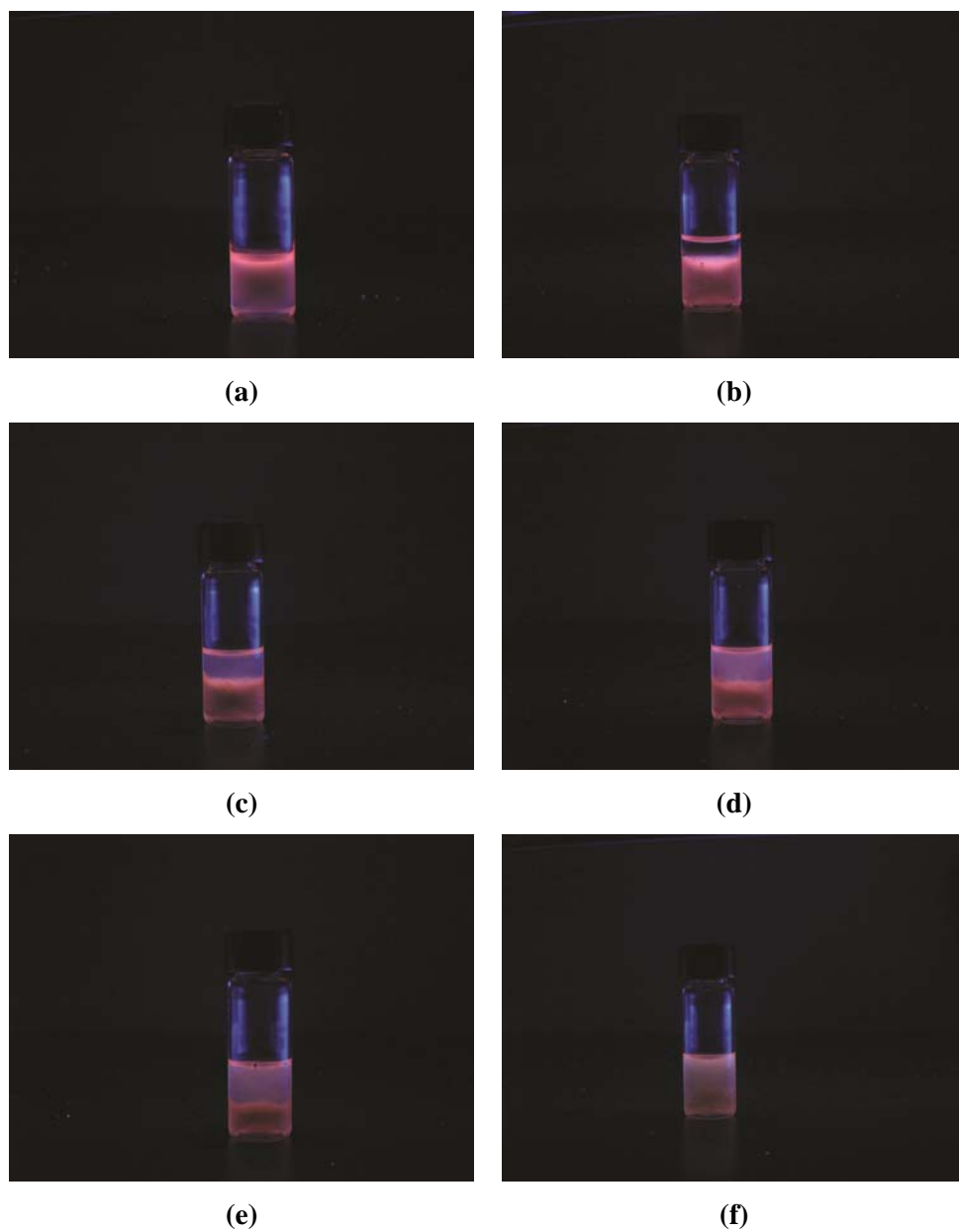


Figure S61. The evolution of photoluminescence of gel containing only Eu(III) upon addition of $(\text{EtO})_3\text{PO}$ on the top of the gel. (a) Original, and (b) 0 min, (c) 30 min, (d) 60 min, (e) 2 h, (f) 5 h after addition of $(\text{EtO})_3\text{PO}$.

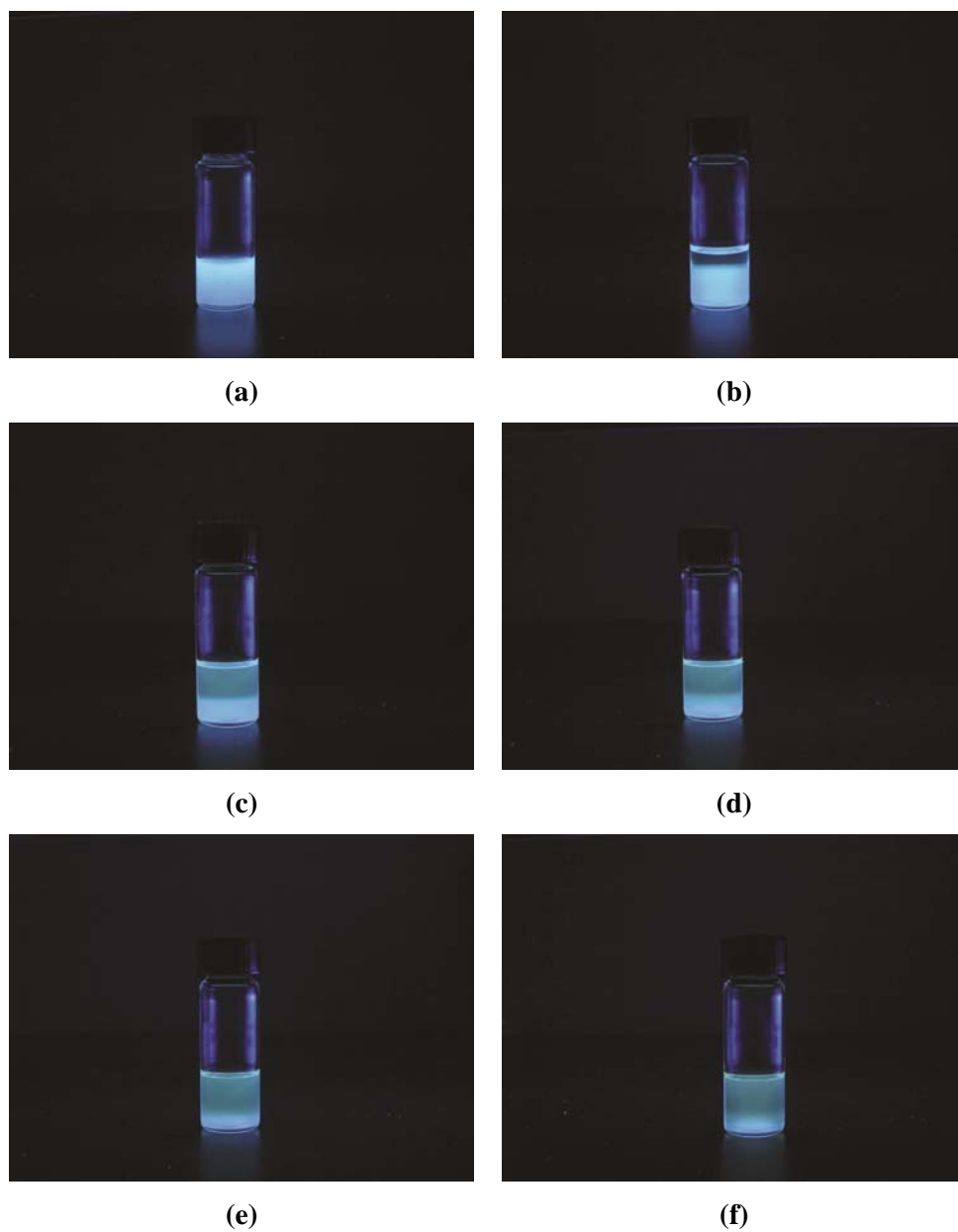


Figure S62. The evolution of photoluminescence of gel containing only Zn(II) upon addition of PMDETA on the top of the gel. (a) Original, and (b) 0 min, (c) 15 min, (d) 30 min, (e) 45 min, (f) 60 min after addition of PMDETA.

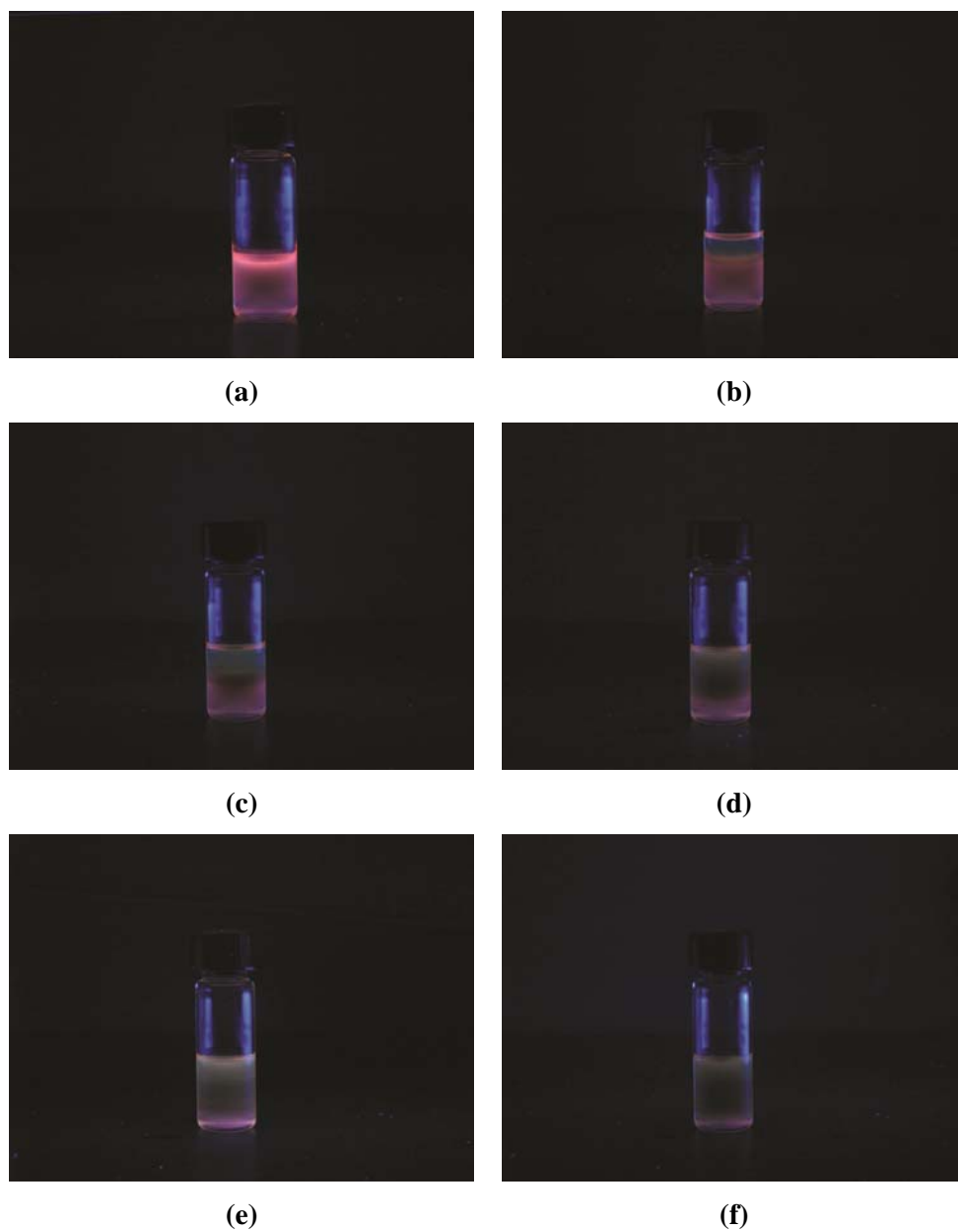


Figure S63. The evolution of photoluminescence of gel containing only Eu(III) upon addition of PMDETA on the top of the gel. (a) Original, and (b) 0 min, (c) 15 min, (d) 30 min, (e) 45 min, (f) 60 min after addition of PMDETA.

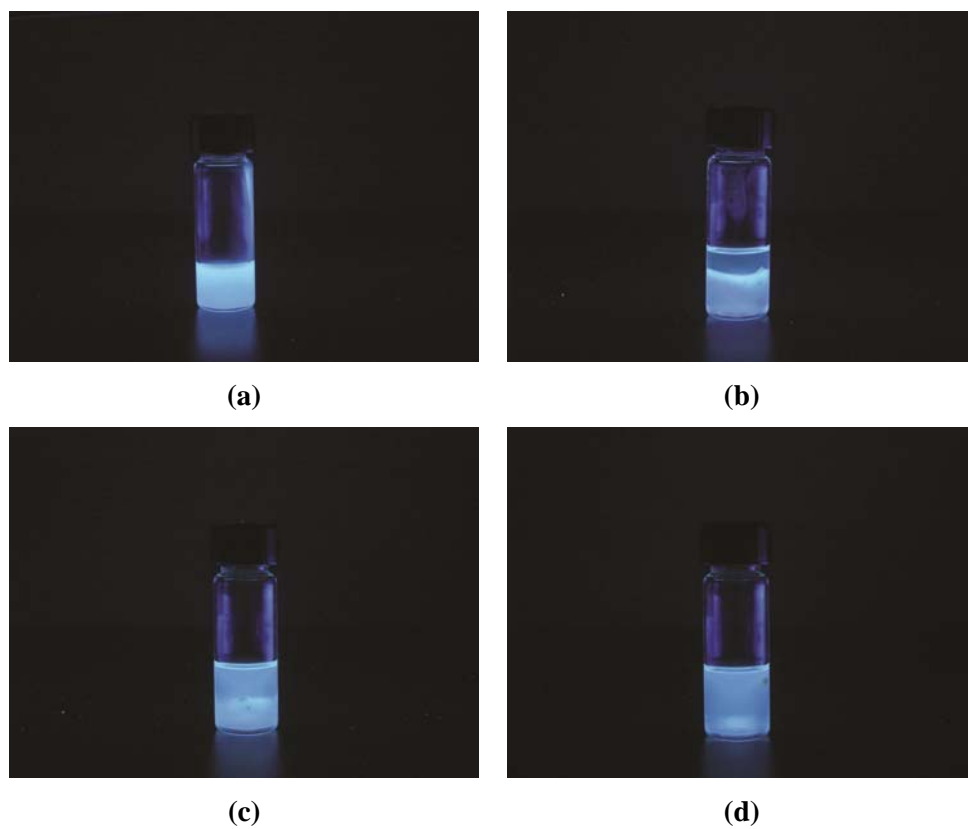


Figure S64. The evolution of photoluminescence of gel containing only Zn(II) upon addition of BPy on the top of the gel. (a) Original, and (b) 0 min, (c) 15 min, (d) 30 min after addition of BPy.

2.11 Self-healing of Gels

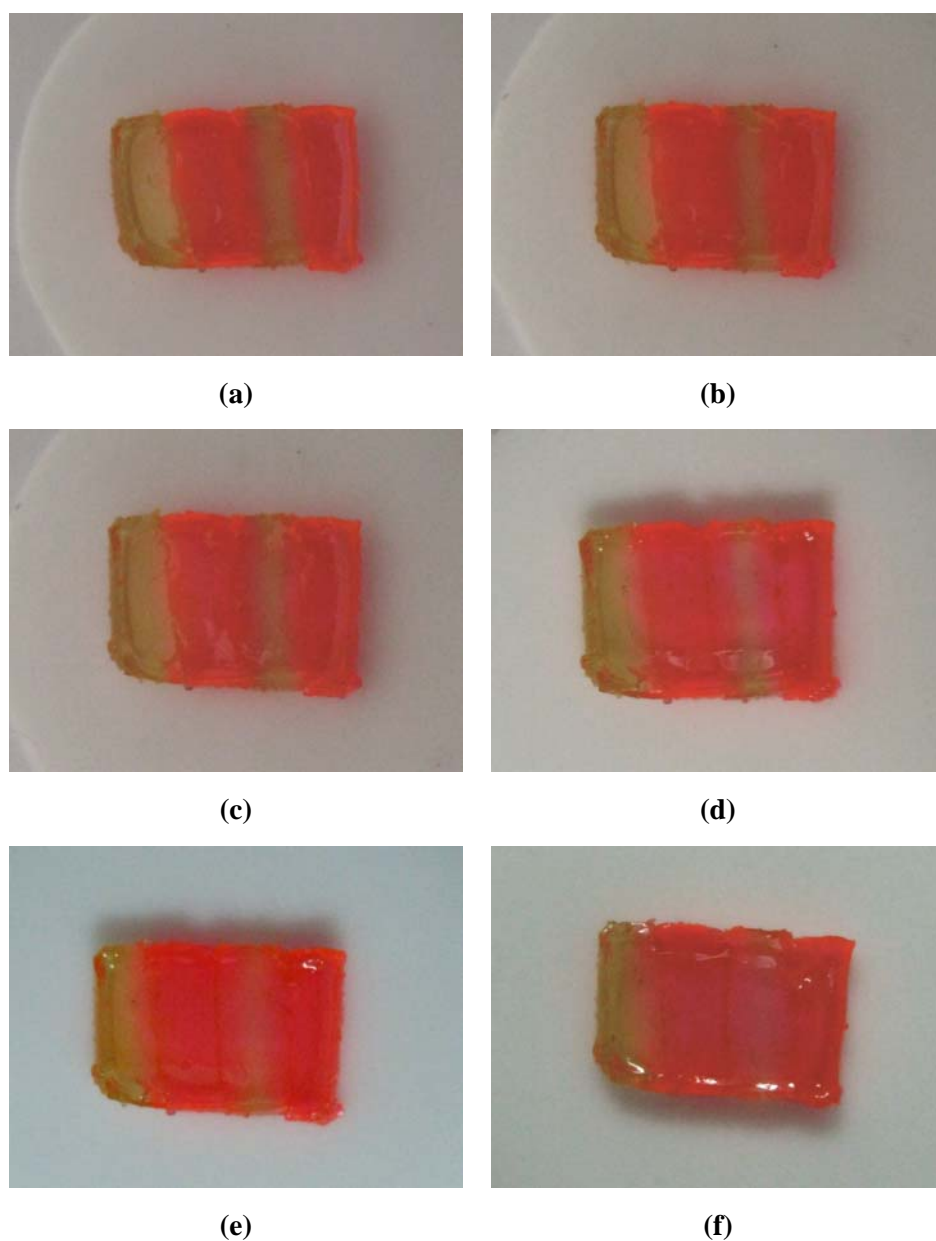


Figure S65. Optical images taken after different time intervals during the self-healing process of a gel sample (100% Eu(III) and no Zn(II), in 1,1,2,2-tetrachloroethane): (a) 1 h, (b) 2 h, (c) 3 h, (d) 4 h, (e) 5 h, (f) 6 h after joining the separated blocks together. A movie showing the stretching of the healed gel is also available. The rhodamine B moved across the fusion interface slowly, demonstrating the exchange of matter between different blocks.

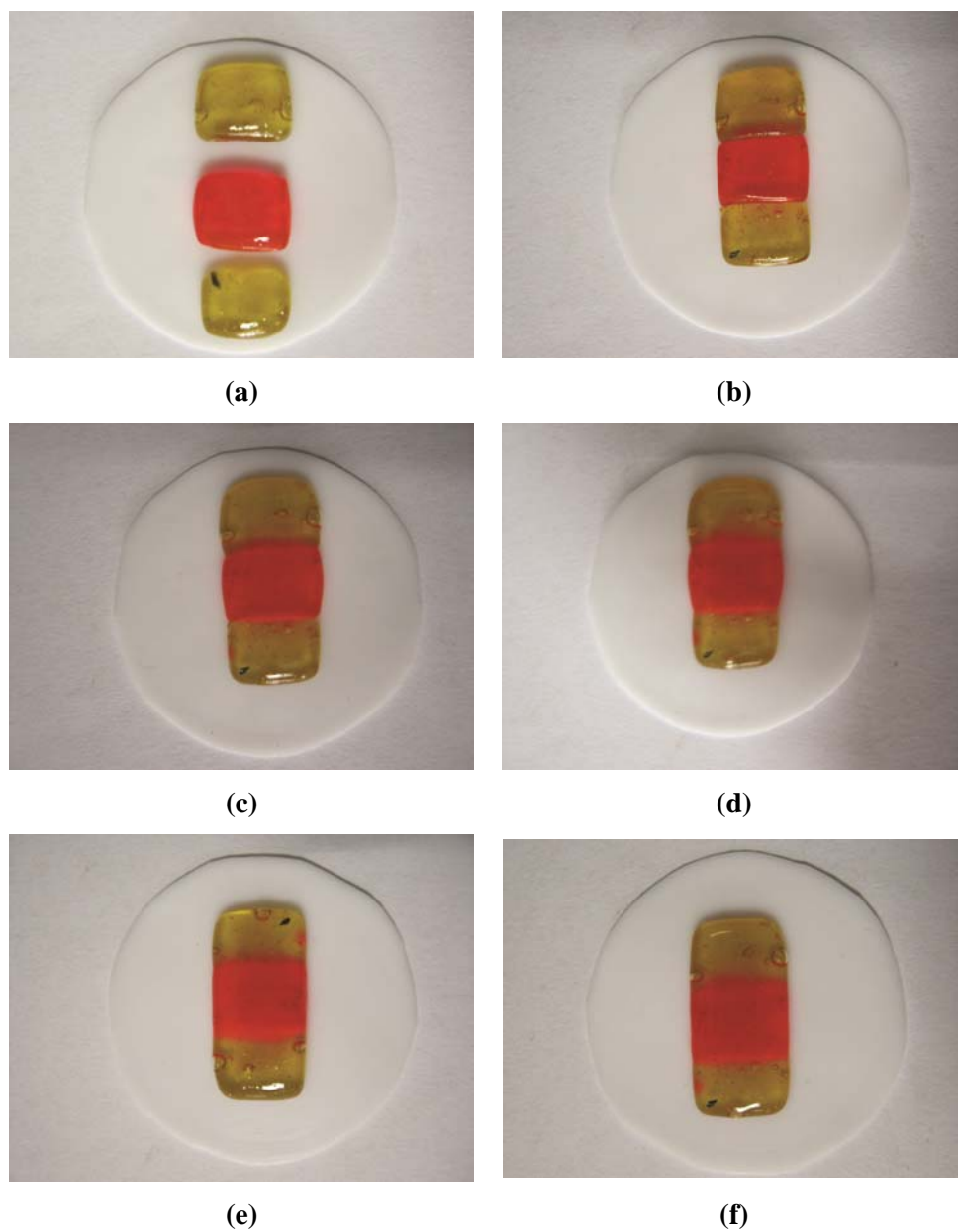


Figure S66. Optical images taken after different time intervals during the self-healing process of a gel sample (75% Zn(II) and 25% Eu(III), in 1,1,2,2-tetrachloroethane): (a) original separated blocks, (b) 0 h, (c) 1 h, (d) 2 h, (e) 3 h, (f) 4 h after joining the separated blocks together.

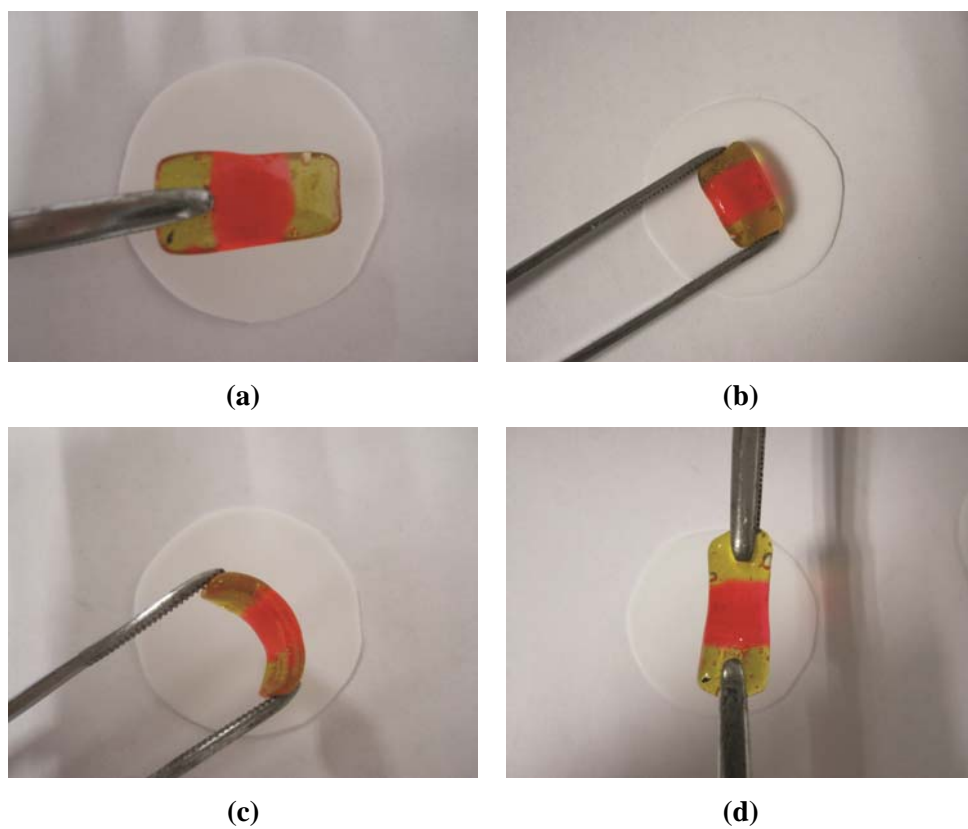


Figure S67. Healed gel (75% Zn(II) and 25 Eu(III), in 1,1,2,2-tetrachloroethane) subjected to different treatments: (a) held horizontally, (b) squeezing, (c) bending, (d) stretching.

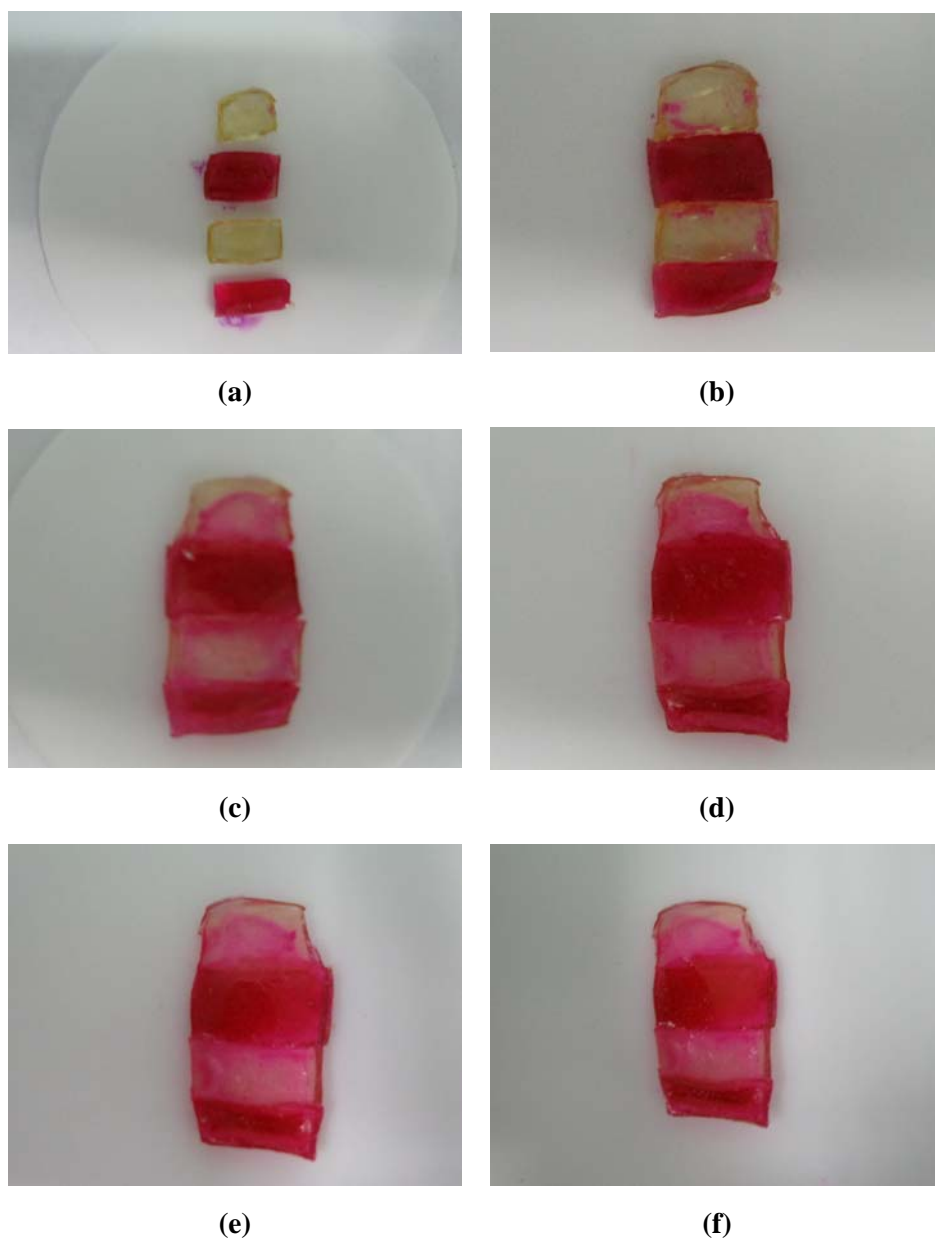


Figure S68. Optical images taken after different time intervals during the self-healing process of a gel sample (100% Eu(III) and no Zn(II), in toluene): (a) original separated blocks, (b) 0 h, (c) 1 h, (d) 2 h, (e) 4 h, (f) 6 h after joining the separated blocks together.

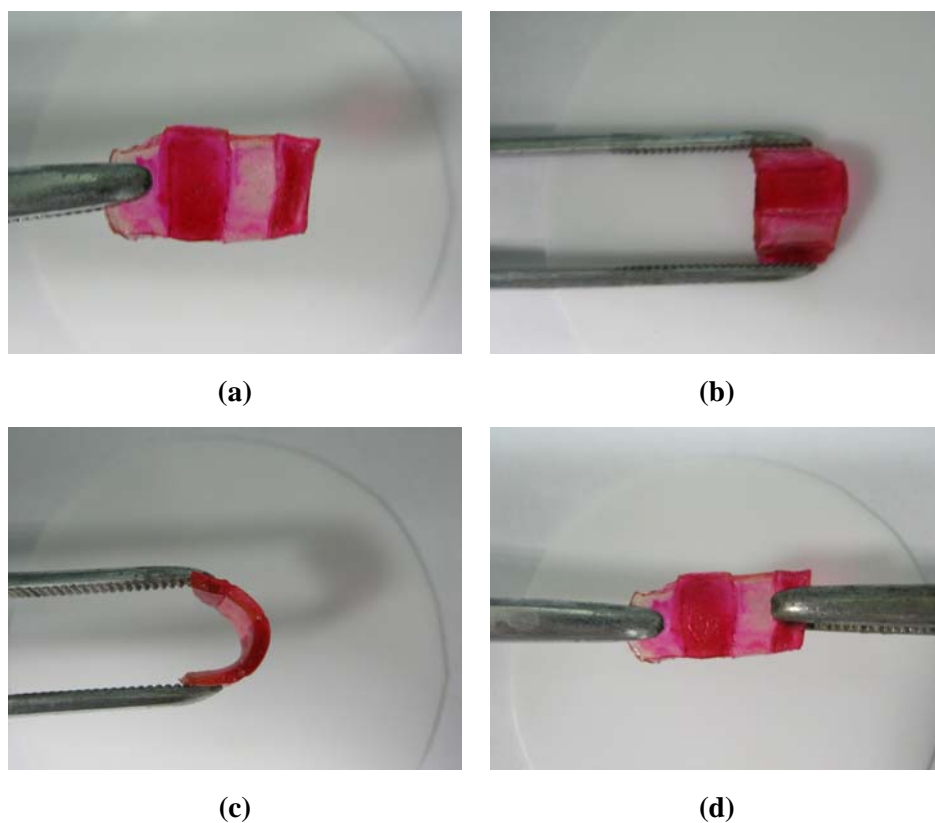


Figure S69. Healed gel (100% Eu(III) and no Zn(II), in toluene) subjected to different treatments: (a) held horizontally, (b) squeezing, (c) bending, (d) stretching.

Video: Stretching of the healed gel (in in 1,1,2,2-tetrachloroethane) containing 100% Eu(III) and no Zn(II).

References:

- [1] a) B. A. Dana, B. H. Robinson, and J. Simpson, *J. Organomet. Chem.* **2002**, *648*, 251-; b) R. M. Meudtner, S. Hecht, *Macromol. Rapid Commun.* **2008**, *29*, 347-351; c) R. M. Meudtner, M. Ostermeier, R. Goddard, C. Limberg, S. Hecht, *Chem. Eur. J.* **2007**, *13*, 9834-9840; d) J. T. Fletcher, B. J. Bumgarner, N. D. Engels, D. A. Skoglund, *Organometallics* **2008**, *27*, 5430-5433; e) E. Brunet, O. Juanes, L. Jiménez, J. C. Rodríguez-Ubis, *Tetrahedron Lett.* **2009**, *50*, 5361-5363.
- [2] a) A. J. Scheel, H. Komber, B. I. Voit, *Macromol. Rapid Commun.* **2004**, *25*, 1175-; b) V.

Aucagne, K. D. Hänni, D. A. Leigh, P. J. Lusby, D. B. Walker, *J. Am. Chem. Soc.* **2006**, *128*, 2186-.

- [3] a) U. S. Schubert, C. Eschbaumer, C. H. Weidl, *Des. Monom. Polym.* **1999**, *2*, 185-198; b) Z. Guan, J. T. Roland, J. Z. Bai, S. X. Ma, T. M. McIntire, M. Nguyen, *J. Am. Chem. Soc.* **2004**, *126*, 2058-2065; c) L. T. James Korley, B. D. Pate, E. L. Thomas, P. T. Hammond, *Polymer* **2006**, *47*, 3073-3082.